AD-744 868

AD

0058-8

[illegible] FOR DISTANCE MEASURING SYSTEMS [illegible]

L. R. Couch

March 28, 1972

Prepared for:

U. S. Army Materiel Command

HARRY DIAMOND LABORATORIES

Washington, D. C. 20438

Under contract number
DAAG39-70-C-0058

Security Classification AD744483

DOCUMENT CONTROL DATA - R & D

(Security classification of title, body of abstract and indexing annotation must be entered when the overall report is classified)

1. ORIGINATING ACTIVITY (Corporate author)
ENGINEERING AND INDUSTRIAL EXPERIMENT STATION
UNIVERSITY OF FLORIDA
GAINESVILLE, FLORIDA 32601

2a. REPORT SECURITY CLASSIFICATION
UNCLASSIFIED

2b. GROUP

3. REPORT TITLE
RANGE LAWS FOR DISTANCE MEASURING SYSTEMS USING FREQUENCY MODULATION WITH A NONLINEAR TRIANGULAR WAVESHAPE

4. DESCRIPTIVE NOTES (Type of report and inclusive dates)

5. AUTHOR(S) (First name, middle initial, last name)
Leon W. Couch

6. REPORT DATE	7a. TOTAL NO OF PAGES	7b. NO. OF REFS
March 28, 1972	54	6

8a. CONTRACT OR GRANT NO	9a. ORIGINATOR'S REPORT NUMBER(S)
DAAG39-70-C-0058	
b. PROJECT NO. HDL Proj: 16114	0058-8
c. DA-1B262301A208	9b. OTHER REPORT NO(S) (Any other numbers that may be assigned this report) SR-72-3
d. AMCMS Code: 522A.11.17700	

10. DISTRIBUTION STATEMENT
This document has been approved for public release and sale; its distribution is unlimited.

11. SUPPLEMENTARY NOTES	12. SPONSORING MILITARY ACTIVITY
	ARMY MATERIEL COMMAND HARRY DIAMOND LABORATORIES WASHINGTON, D. C. 20438

13. ABSTRACT

Range laws are obtained for a distance measuring system which transmits an RF signal. The RF is frequency modulated by a nonlinear triangular waveform, the amount of nonlinearity being specified by a parameter.

The nonlinearity may have desirable or undesirable effects; that is, the sidelobe level of the range response may be decreased or increased depending on the shape and amount of nonlinearity.

The results of this report may be used to predict range laws of systems which have nonlinear triangular modulation. Alternately, practical nonlinear triangular waveforms may be specified which will reduce the range-law sidelobes.

DD FORM 1 NOV 68 1473 REPLACES DD FORM 1473, 1 JAN 64, WHICH IS OBSOLETE FOR ARMY USE.

A

Security Classification

14 KEY WORDS	LINK A		LINK B		LINK C	
	ROLE	WT	ROLE	WT	ROLE	WT
1. Frequency Modulation	9	0				
2. Nonlinear Triangular Frequency Modulation			8	3		
3. Radar	1	0				
4. Range Laws	9	3				
5. Sidelobe Suppression					8	3
6. Triangle Waveform Modulation	9					

DA-1B262301A208
AMCMS Code: 522A.11.17700
HDL Proj: 16114

AD_____

0058-8

RANGE LAWS FOR DISTANCE MEASURING SYSTEMS USING FREQUENCY MODULATION WITH A NONLINEAR TRIANGULAR WAVESHAPE

by

L. W. Couch

March 28, 1972

United States Army Materiel Command
HARRY DIAMOND LABORATORIES
Washington, D. C. 20438

Prepared by:

ENGINEERING AND INDUSTRIAL EXPERIMENT STATION
College of Engineering
University of Florida
Gainesville, Florida 32601

Under Contract Number
DAAG39-70-C-0058

ABSTRACT

Range laws are obtained for a distance measuring system which transmits an RF signal. The RF is frequency modulated by a nonlinear triangular waveform, the amount of nonlinearity being specified by a parameter.

The nonlinearity may have desirable or undesirable effects; that is, the sidelobe level of the range response may be decreased or increased depending on the shape and amount of nonlinearity.

The results of this report may be used to predict range laws of systems which have nonlinear triangular modulation. Alternately, practical nonlinear triangular waveforms may be specified which will reduce the range-law sidelobes.

TABLE OF CONTENTS

LIST OF FIGURES

LIST OF FIGURES

KEY TO SYMBOLS

B	Peak-to-peak FM deviation (Hz)
c_k	Fourier coefficient of the mixer output for the kth harmonic of the fundamental modulation frequency
D	Deviation sensitivity of the FM modulation (radians/volt-sec)
DMS	Distance measuring system
$m(t)$	Composite frequency modulating waveform
$100P_c$	Percent cube-law nonlinearity
$100P_s$	Percent sinusoidal nonlinearity
$100P_t$	Percent of pure triangular contribution to the composite nonlinear triangular modulating waveform
$R_k(\tau)$	Range law associated with the kth harmonic of the fundamental modulation frequency
T	Period of the modulation
$v(t) = e^{j\int_0^t m(\tau)d\tau}$	Complex envelope of the transmitted RF signal
$x = 2B\tau$	Normalized round-trip time delay between the distance measuring-device and the target
$x_0 = 2B\tau_0$	Normalized round-trip time delay which gives the peak range law response
$y(t,\tau)$	Mixer output signal
$\theta_d(t,\tau)$	Difference phase between the transmitted and received RF signals
τ	Round-trip time delay between the distance-measuring-device and the target
$\omega_c = 2\pi f_c$	Radian carrier frequency
$\omega_d = 2\pi f_d$	Radian doppler frequency
$\omega_{id}(t,\tau) = \frac{d\theta_d(t,\tau)}{dt}$	Instantaneous difference frequency (rad/sec) between the transmitted and received RF signals
$\omega_m = 2\pi f_m = \frac{2\pi}{T}$	Fundamental modulating frequency (rad/sec)

RANGE LAWS FOR DISTANCE MEASURING SYSTEMS USING FREQUENCY MODULATION WITH A NONLINEAR TRIANGULAR WAVESHAPE

1. INTRODUCTION

The range law of a distance-measuring system (DMS) is the envelope of the test statistic [1]. This is a function of the time delay between the device and the target (or the corresponding distance between the device and the target). If this envelope is above a certain level determined by a pre-set threshold, the device is said to be within the functioning window of the target and an alarm signal is given at the output of the threshold device. Here the DMS is assumed to be of the type that is frequency modulated by a periodic waveform.

It is well-known that nonlinear frequency modulation can be used to decrease the sidelobe levels in the range law [2, Chapter 20],[6]. In fact, by frequency modulating with a waveform having Taylor weighing, the sidelobe may be decreased to 40dB below the main lobe, as compared to 13dB sidelobe suppression for pure triangular modulation [2]. The modulating waveform for Taylor weighing is

$$m(t) = a\left(\frac{t}{T} + \sum_{n=1}^{7} K_n \sin(n\omega_m t)\right), \quad |t| < \frac{T}{2}$$

where T is the period of the modulation and $\omega_m = 2\pi/T$. For the DC range-law to have 40dB sidelobe suppression, the constants are $K_1 = -0.1145$, $K_2 = 0.0396$, $K_3 = -0.0202$, $K_4 = 0.0118$, $K_5 = -0.0082$, $K_6 = 0.0055$ and $K_7 = -0.0040$ [2]. In practice this modulating waveform is difficult to generate.

In this report the range laws for the DMS will be calculated for a class of nonlinear frequency modulating waveforms. This class consists of (1) Triangle plus one sinusoidal term and (2) Triangle plus a cube-law term. This class of waveforms is relatively easy to generate in practice. Thus, the results of this report can be used to design practical nonlinear modulating waveforms which will increase the sidelobe suppression over that obtained by use of pure triangular modulation. Alternately, this class of waveforms can be used to model the actual nonlinear modulation in devices which are designed to have pure triangular modulation. Thus, the realized sidelobe suppression of an actual DMS with "triangular" modulation can be predicted. This is important because, for certain nonlinear shapes, the sidelobe suppression is increased (instead of decreased) by the incidental nonlinearity.

2. GENERAL FORMULATION FOR THE RANGE LAW

2.1 Range Law in Terms of the Fourier Coefficients

For periodic modulation the range law is obtained by evaluating the Fourier coefficient for the mixer output of the DMS. Referring to Figure 1,

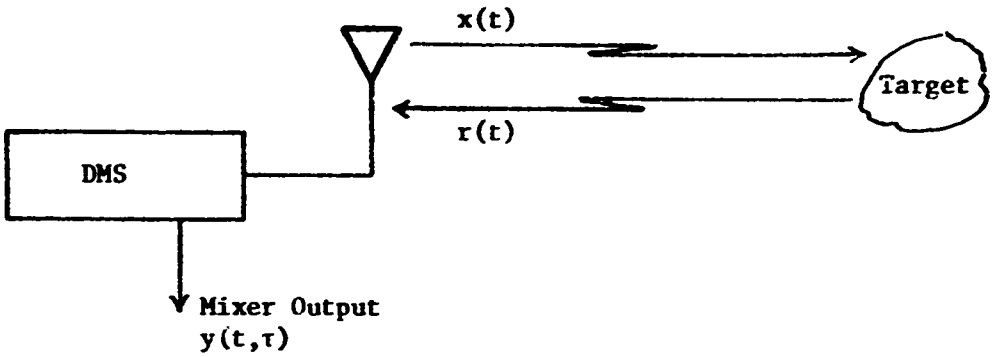

Figure 1. DMS and a Point Target

the transmitted signal is represented by

$$x(t) = \sqrt{2}\ \mathrm{Re}\ \{v(t)e^{j\omega_c t}\} \tag{1}$$

where ω_c is the radian carrier frequency and $v(t)$ is the complex envelope [3]. Then the corresponding received signal is

$$r(t) = \sqrt{2}\ \mathrm{Re}\ \{v(t-\tau)e^{j\omega_c(t-\tau)}\} \tag{2}$$

where τ is the round-trip time delay.
To the first approximation, the mixer output is given by the cross-product term

$$\begin{aligned} y(t,\tau) &= x(t)r(t) \\ &= \mathrm{Re}\ \{v(t)v^*(t-\tau)e^{j\omega_c\tau}\} \\ &\quad + \mathrm{Re}\ \{v(t)v(t-\tau)e^{j\omega_c(2t-\tau)} \end{aligned}$$

where $[\cdot]^*$ denotes the complex conjugate of $[\cdot]$.
Neglecting the output about $2\omega_c$ (which is filtered out in the physical DMS), we have for the mixer output

$$y(t,\tau) = \mathrm{Re}\ \{v(t)v^*(t-\tau)e^{j\omega_c\tau}\} \quad . \tag{3}$$

The test statistic is a filtered version of (3) usually obtained by a doppler band-pass filter centered about some harmonic of the fundamental modulating frequency.

For this frequency modulated DMS

$$v(t) = e^{j[D_0 \int^t m(t)dt]}$$

where D is the deviation sensitivity (radians/volt-sec) and m(t) is the periodic frequency modulating waveform. Then

$$v(t)v^*(t-\tau) = e^{j\theta_d(t,\tau)} \tag{4}$$

where

$$\theta_d(t,\tau) = D \int_{t-\tau}^{t} m(\sigma)d\sigma \ .$$

$\theta_d(t,\tau)$ is the mixer output difference phase with τ being a parameter.

The instantaneous difference radian frequency associated with the mixer output is then

$$\omega_{id}(t,\tau) = \frac{d\theta_d(t,\tau)}{dt} = D[m(t) - m(t-\tau)] \tag{5}$$

where it is assumed that the variation of τ with respect to t is negligible, i.e. the doppler frequency is much less than the carrier frequency. Thus,

$$\boxed{\theta_d(t,\tau) = D \int_0^t [m(t) - m(t-\tau)]d\tau} \tag{6}$$

If m(t) is periodic, then, $\theta_d(t,\tau)$ is periodic with respect to t. Thus, from (4), $v(t)v^*(t-\tau)$ is also periodic and can be expanded in a Fourier series

$$v(t)v^*(t-\tau) = e^{j\theta_d(t,\tau)} = \sum_{k=-\infty}^{k=\infty} c_k e^{jk\omega_m t} \tag{7}$$

where

$$c_k = \frac{1}{T} \int_0^T e^{j\theta_d(t,\tau)} \ e^{-jk\omega_m t} \ dt \tag{8}$$

$$\omega_m = \frac{2\pi}{T}$$

and T is the period of the modulating waveform.

Using the above formulation the mixer output can be obtained in terms of the Fourier coefficients $\{c_k\}$. Assuming a modulating waveform such that the instantaneous difference frequency has half-wave odd symmetry; that is

$$\boxed{\omega_{id}(t,\tau) = -\omega_{id}(t + \frac{T}{2} \ , \ \tau)} \ ,$$

then from Appendix A, it follows that the mixer output is

$$y(t,\tau) = |c_0(\tau)| \cos [\omega_d(t-t_0) + \angle c_0] + \sum_{k=1}^{\infty} 2|c_k(\tau)| \cos [\omega_d(t-t_0) + \angle c_k] \cos [k\omega_m(t-t_0)] \quad (9)$$

where

t_0 is the value of t at the first turn-around time of the modulation m(t),

$|[\cdot]|$ denotes the magnitude of $[\cdot]$

and

$\angle[\cdot]$ denotes the angle of $[\cdot]$.

The range law is given by the envelope of the output of the doppler-band filter centered at $\omega = k\omega_m$. Thus, the range laws are

$$R_k(\tau) = \begin{cases} |c_0(\tau)| , & k = 0 \\ 2|c_k(\tau)| , & k = 1, 2, \ldots \end{cases} \quad (10)$$

where

$$c_k(\tau) = \frac{1}{T} \int_0^T e^{j\theta_d(t,\tau)} e^{-jk\omega_m t} dt \quad . \quad (11)$$

2.2 Relationship Between the Fourier Coefficients and the Ambiguity Function

It is interesting to relate $c_k(\tau)$ with the Ambiguity Function. The Ambiguity Function is given by [1, p. 353]

$$\lambda(\tau,w) \triangleq \int_{-\infty}^{\infty} v(t - \tfrac{1}{2}\tau)v^*(t + \tfrac{1}{2}\tau)e^{-jwt} dt$$

which becomes for periodic complex envelopes

$$\lambda(\tau,w) = \frac{1}{T} \int_0^T v(t - \tfrac{1}{2}\tau)v^*(t + \tfrac{1}{2}\tau)e^{-jwt} dt \quad . \quad (12)$$

Using (7), (11) and (12) we obtain the relationship

$$c_k(\tau) = e^{-jk\frac{\omega_m\tau}{2}} \lambda(-\tau, k\omega_m) \quad (13)$$

or

$$\boxed{|c_k(\tau)| = |\lambda(-\tau, k\omega_m)|} \tag{14}$$

Thus, the magnitude of the Fourier coefficient gives the magnitude of the Ambiguity Function along the $w = k\omega_m$ axis where the positive and negative directions of the τ axis have been reversed.

Furthermore, the Fourier coefficient corresponding to the DC range law, $c_0(\tau)$, is related to the power spectrum of the transmitted signal by the Fourier transform. From (12) for the case of $w = 0$, $\lambda(\tau,0)$ is the autocorrelation, $R_v(\tau)$, of the complex envelope $v(t)$ of the transmitted RF signal, $x(t)$. That is, for $w = 0$, (13) becomes

$$R_v(\tau) = c_0(-\tau) = \lambda(\tau,0)$$

and

$$R_v^*(\tau) = R_v(-\tau).$$

The power spectrum of the transmitted signal is given by [3]

$$P_x(\omega) = \frac{1}{4}\left[P_v(\omega-\omega_0) + P_v(-\omega-\omega_0)\right] .$$

$P_v(\omega)$ and $R_v(\tau)$ are a Fourier transform pair. Thus

$$c_0(\tau) = \lambda^*(\tau,0) = \frac{1}{2\pi}\int_{-\infty}^{\infty} P_v(\omega)e^{j\omega(-\tau)}\, d\omega$$

or

$$\boxed{c_0(\tau) = \lambda^*(\tau,0) = \frac{2}{\pi}\int_{-B/2}^{B/2} P_x(\omega+\omega_c)e^{-j\omega\tau}\, d\omega} \tag{15}$$

where

$P_x(\omega)$ is the power spectrum of the transmitted RF signal, $x(t)$.

B is the bandwidth (rad/sec) of the RF signal

ω_c is the carrier frequency (rad/sec).

Thus, the $c_0(\tau)$ coefficient, corresponding to the DC range law and the conjugate of the Ambiguity Function evaluated along the w = 0 axis are related to the translated power spectrum of the RF signal by the Fourier transform times $2/\pi$.

A detailed discussion of the Ambiguity Function and its application to DMS is given by Rihaczek [4].

3. RANGE LAW FOR TRIANGLE PLUS SINUSOIDAL NONLINEARITY

The range laws, $R_k(\tau)$, will now be evaluated assuming periodic modulation by a composite waveform which is the sum of a pure triangle plus a sinusoid as shown in Figure 2 below. The composite modulation is described by

$$m(t) = m_1(t) - b \cos \omega_m t \tag{16}$$

where

$$m_1(t) = \begin{bmatrix} a(t - T/4) & , \quad 0 \le t \le T/2 \\ a(t - 3/4\ T) & , \quad T/2 \le t \le T \end{bmatrix} \tag{17}$$

a and b are constants to be determined according to the percentage of sinusoidal nonlinearity.

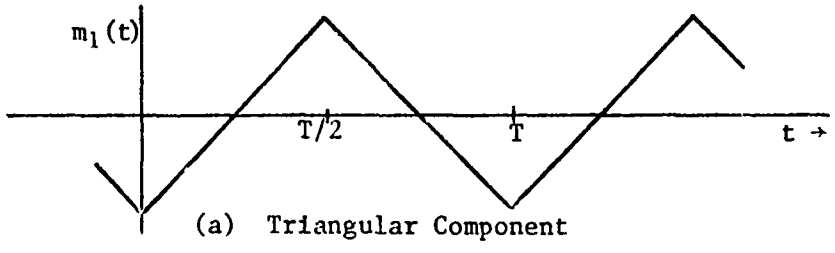

(a) Triangular Component

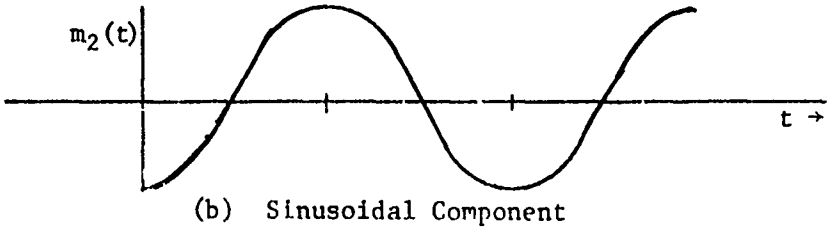

(b) Sinusoidal Component

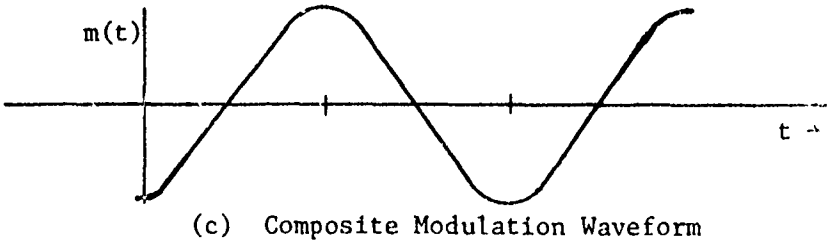

(c) Composite Modulation Waveform

Figure 2. Triangle Plus Sinusoidal Nonlinearity

The percentage of sinusoidal nonlinearity added to the pure triangle component is defined by the percentage of sinusoidal contribution to the composite peak value measured at the time that the peak-value occurs. Thus, the percent sinusoidal nonlinearity is given by $100P_s$ where

$$P_s \triangleq \frac{b}{b + aT/4} \tag{18}$$

The percentage of modulation, see (18), may be positive or negative depending on the sign of b with respect to a. It will be found that the sidelobes of the range law are increased or decreased depending on the sign of P_s.

The range laws resulting from this triangle plus sinusoidal nonlinearity are described by (see Appendix B for the derivation)

$$R_k(\tau) = \begin{cases} |c_0(\tau)| \ , & k = 0 \\ 2|c_k(\tau)| \ , & k = 1,2 \ \ldots \end{cases} \tag{19}$$

where

$$c_k = \frac{1}{2} e^{j(\pi/2)P_s x} \left\{ Y\left[\left(\frac{\pi}{2} P_s x\right) \ , \ (k - xP_t)\right] + (-1)^k e^{j\pi P_t x} Y\left[\left(-\frac{\pi}{2} P_s x\right) \ , \ (k + xP_t)\right] \right\} \tag{20}$$

and

$$Y[z,\nu] \triangleq \frac{1}{\pi} \int_0^{\pi} e^{-j[z \cos\theta + \nu\theta]} d\theta \tag{21}$$

$$x \triangleq 2B\tau \tag{22}$$

$$P_t \triangleq 1 - P_s \tag{23}$$

and B is the peak-to-peak frequency deviation (Hz) of the composite frequency modulating waveform. For $B >> f_m$, which is usually the case, B corresponds to the spectral bandwidth (Hz) of the transmitted RF signal.

For the case of $P_s = 0$, i.e., pure triangular modulation, (20) reduces to

$$c_k = \frac{1}{2} e^{j\frac{\pi}{2}(x-k)} \left\{ \frac{\sin\left[\frac{\pi}{2}(x-k)\right]}{\frac{\pi}{2}(x-k)} + (-1)^k \frac{\sin\left[\frac{\pi}{2}(x+k)\right]}{\frac{\pi}{2}(x+k)} \right\} \tag{24}$$

which yields the well-known [5] sin z/z type of range law.

For the case $P_s = 1.0$, i.e. pure sinusoidal modulation, (20) reduces to

$$c_k = (-1)^k e^{j\frac{\pi}{2}x} J_k\left(\frac{\pi}{2}x\right) \qquad (25)$$

which yields the well-known [2] Bessel function range law.

The range laws for several percentages of sinusoidal nonlinearity are shown in Figures 3-16. These curves were obtained by evaluating (20) numerically.

Figures 3-9 give the range laws for positive percentage of modulation. It is evident that this type of nonlinearity moves the range laws to the left; that is, it decreases the normalized delay, x_0, to the peak of the range law. This positive percentage of sinusoidal nonlinearity also increases the sidelobe level over that obtained for pure triangle modulation for distances larger than x_0. This type of nonlinearity is undesirable.

Figures 10-16 give the range laws for negative percentages of modulation. This type of nonlinearity moves the range laws to the right, i.e. increases x_0. However, the sidelobe level is decreased for distances greater than x_0. From these figures, the optimum decrease in the sidelobe level is obtained when the percentage of sinusoidal nonlinearity is set to approximately

$$P_s = -1.5\ (1/k+4) \quad . \qquad (26)$$

This type of linearily is desirable.

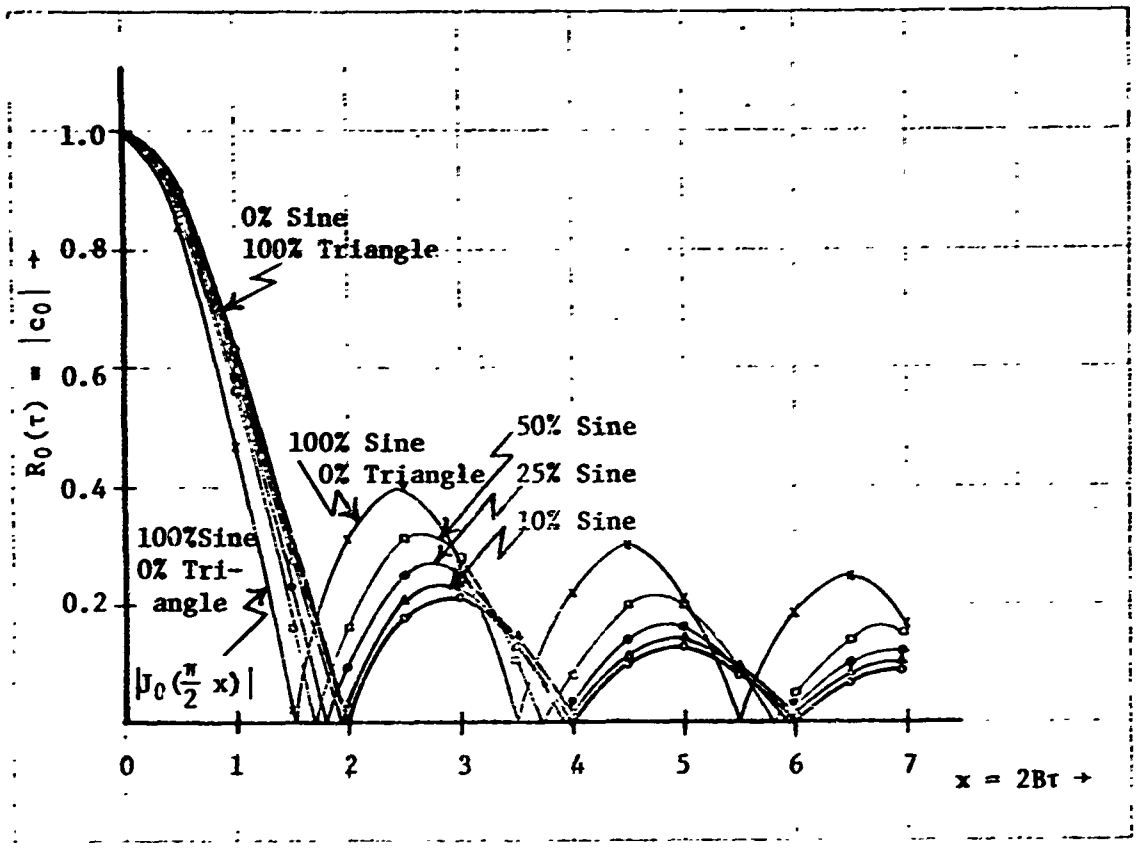

Figure 3. Range Response for K = 0
Sinusoidal Nonlinearity

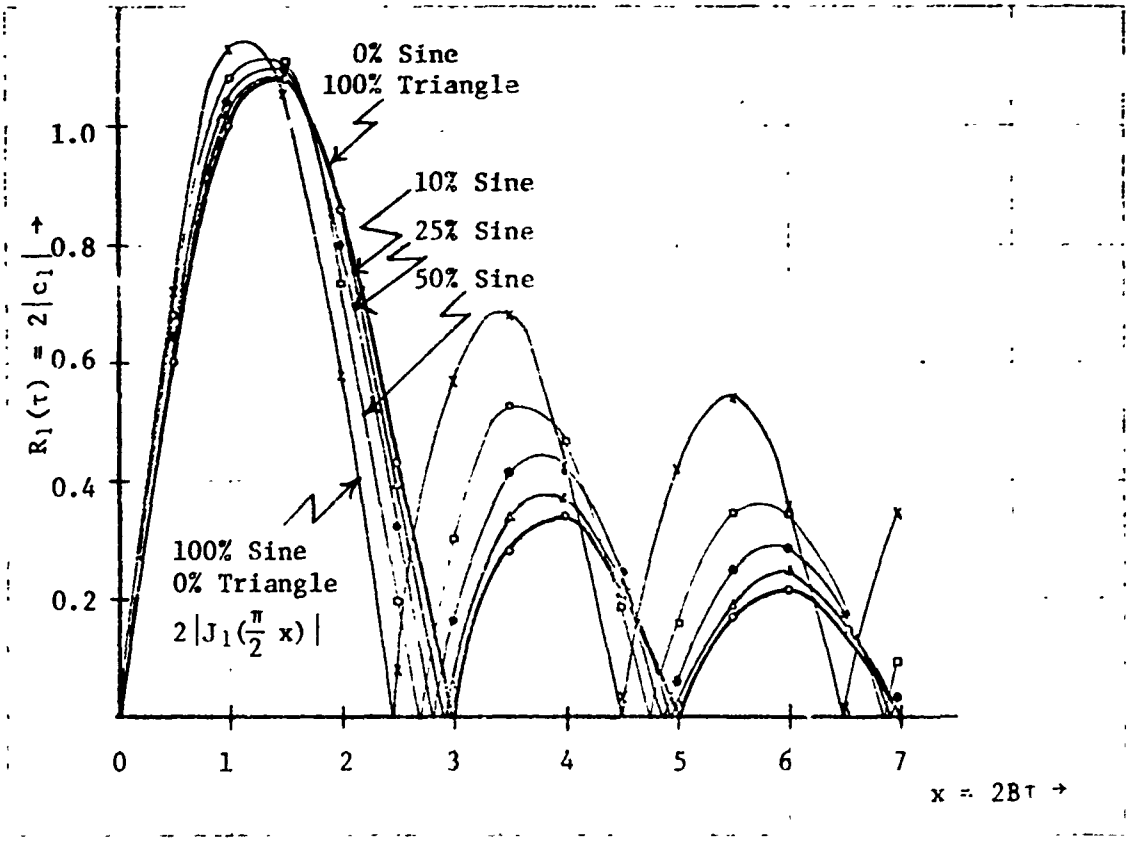

Figure 4. Range Response for K = 1
Sinusoidal Nonlinearity

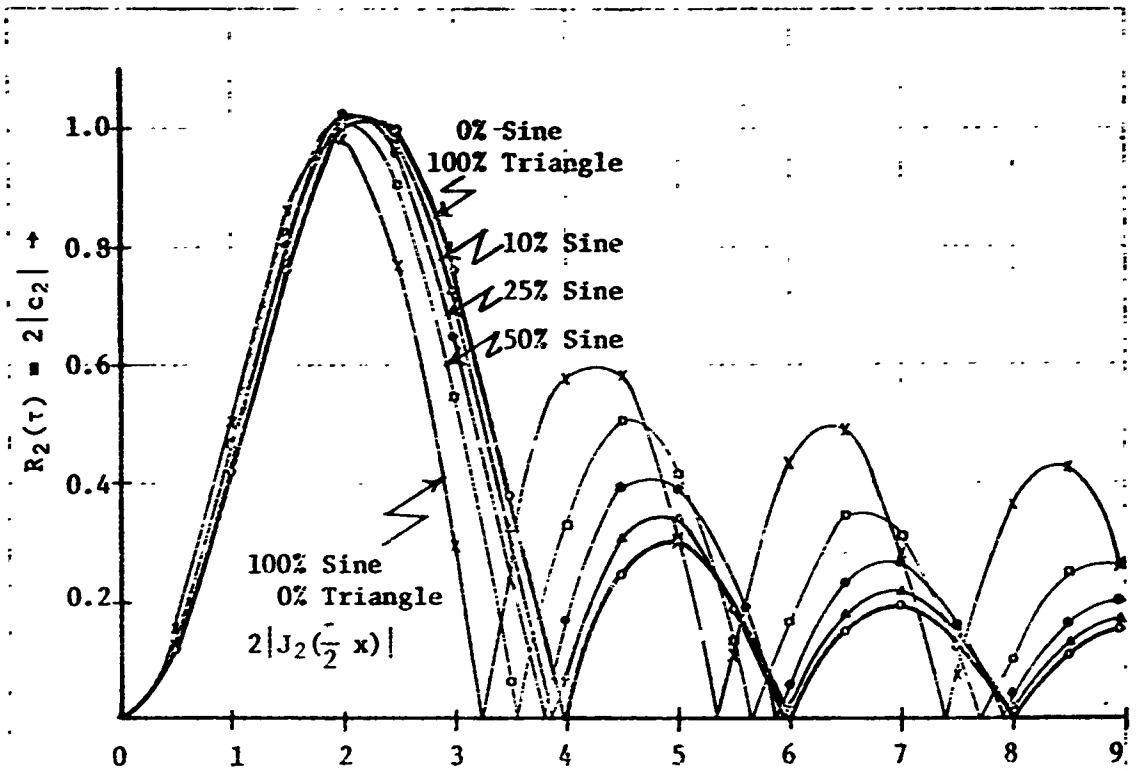

Figure 5. Range Response for K = 2 Sinusoidal Nonlinearity

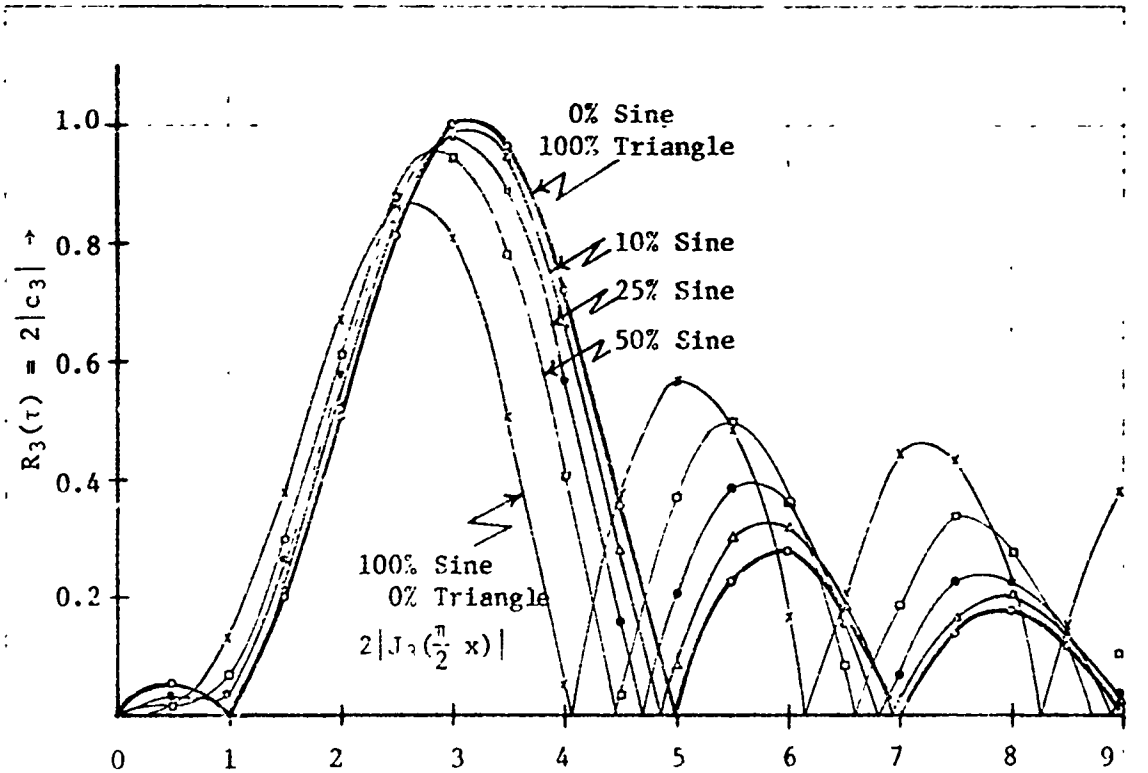

Figure 6. Range Response for K = 3 Sinusoidal Nonlinearity

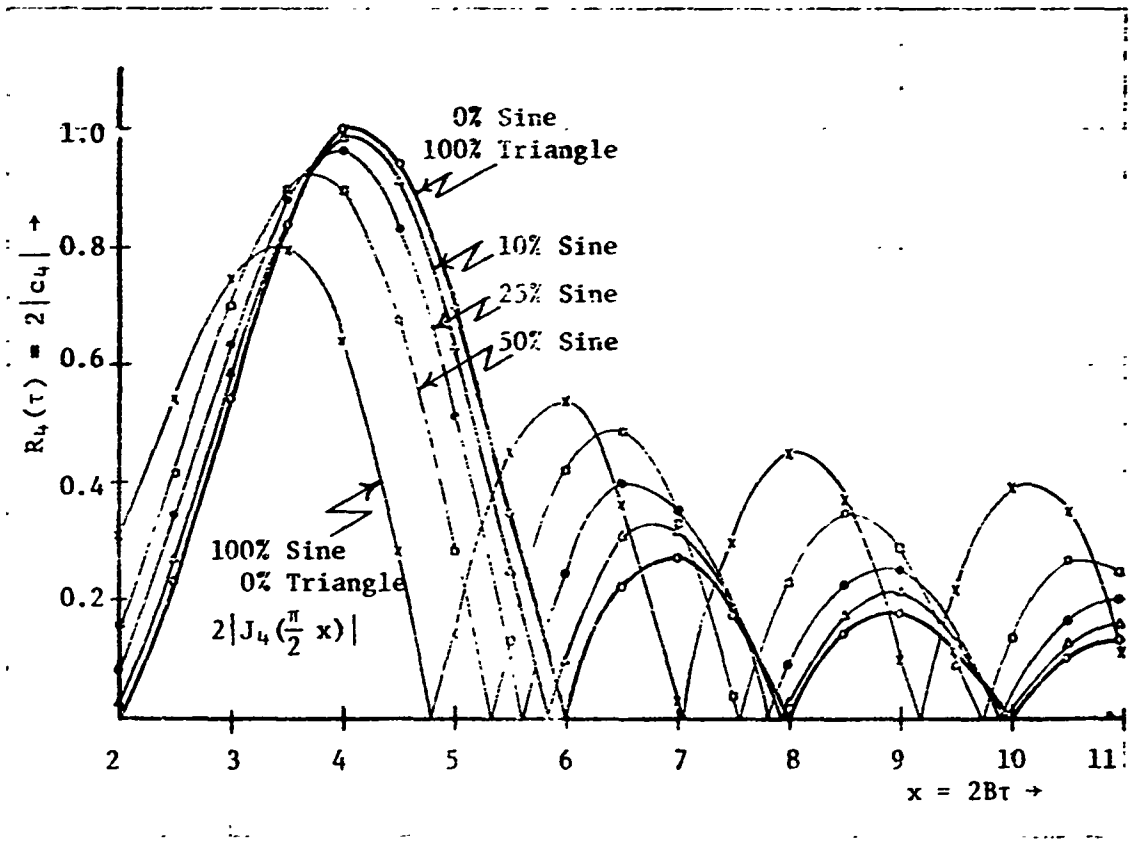

Figure 7. Range Response for K = 4 Sinusoidal Nonlinearity

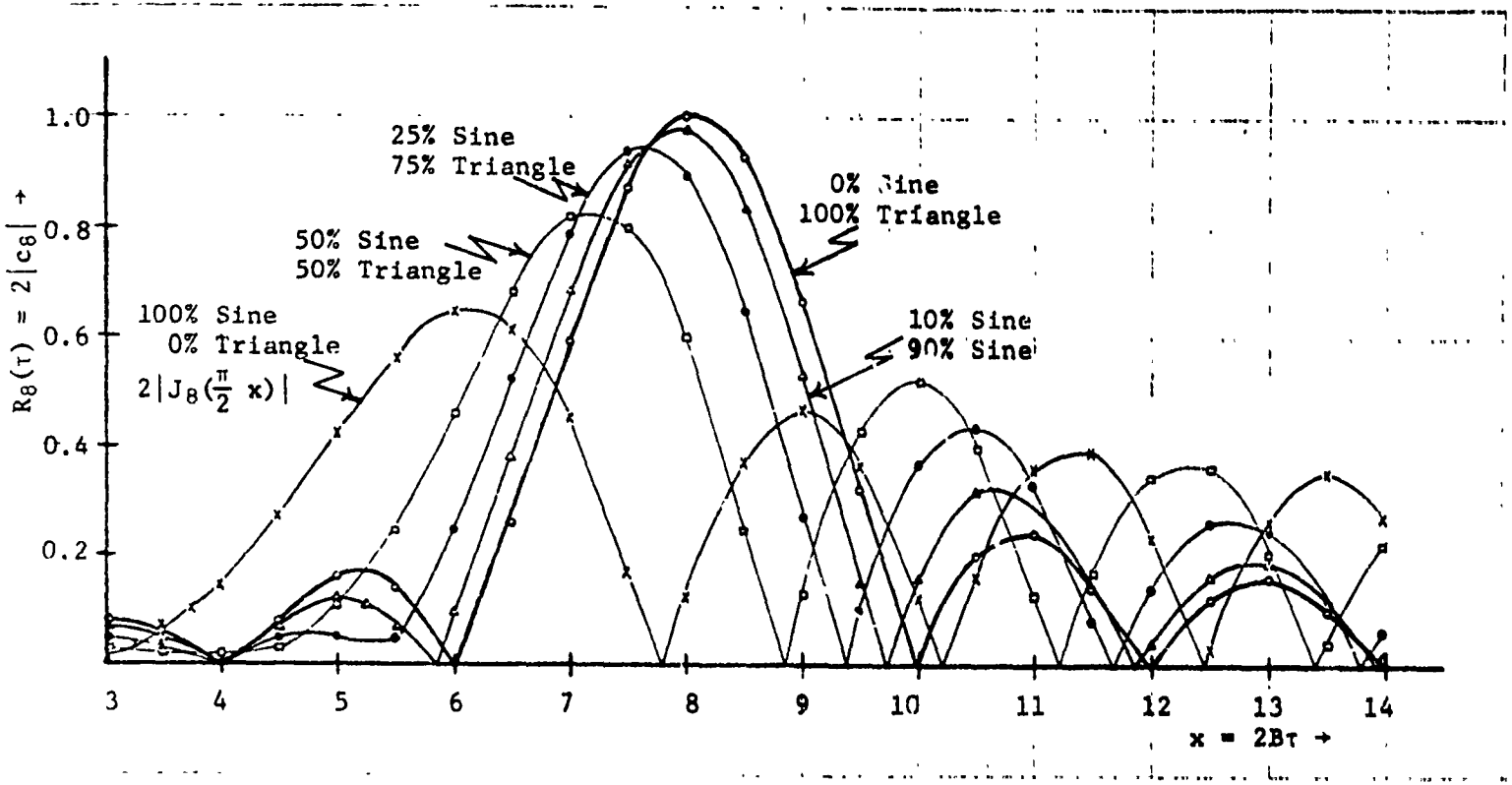

Figure 8. Range Response for K = 8
Sinusoidal Nonlinearity

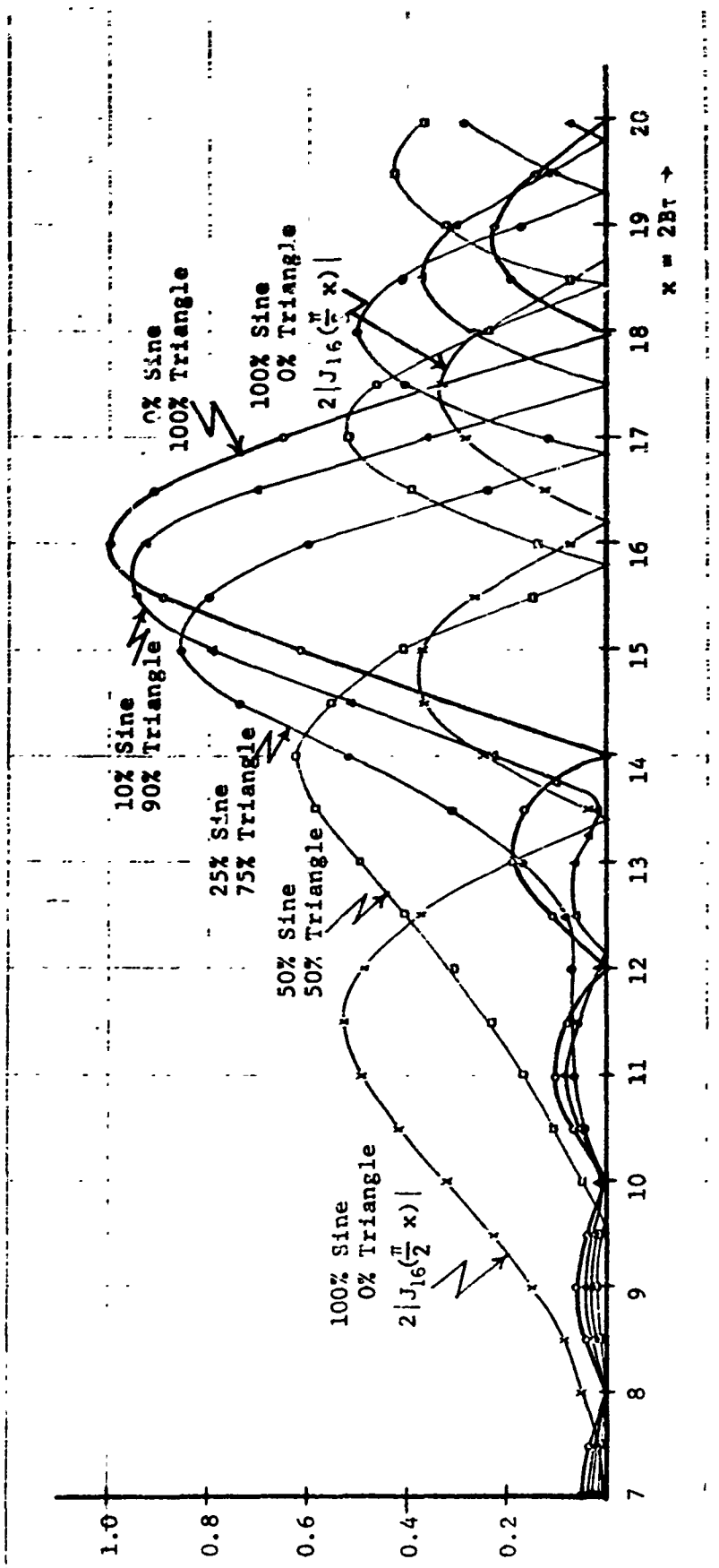

Figure 9. Range Response for K = 16
Sinusoidal Nonlinearity

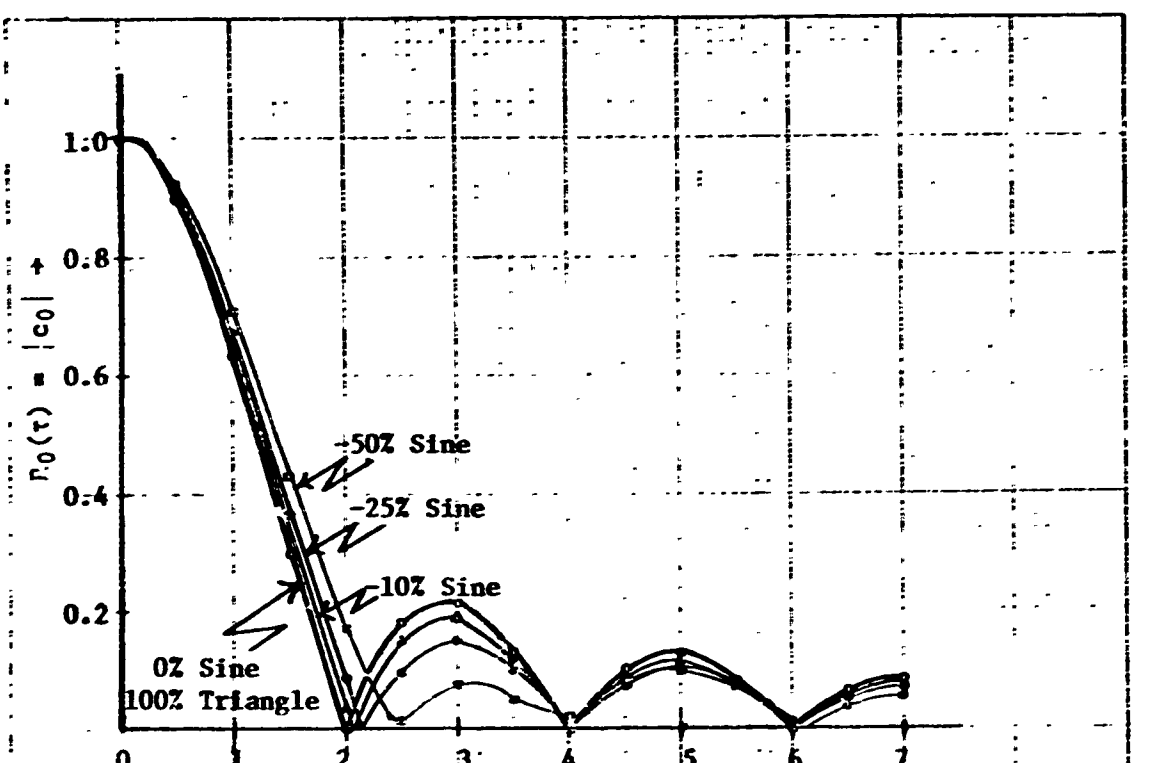

Figure 10. Range Response for K = 0
Negative Sine Nonlinearity

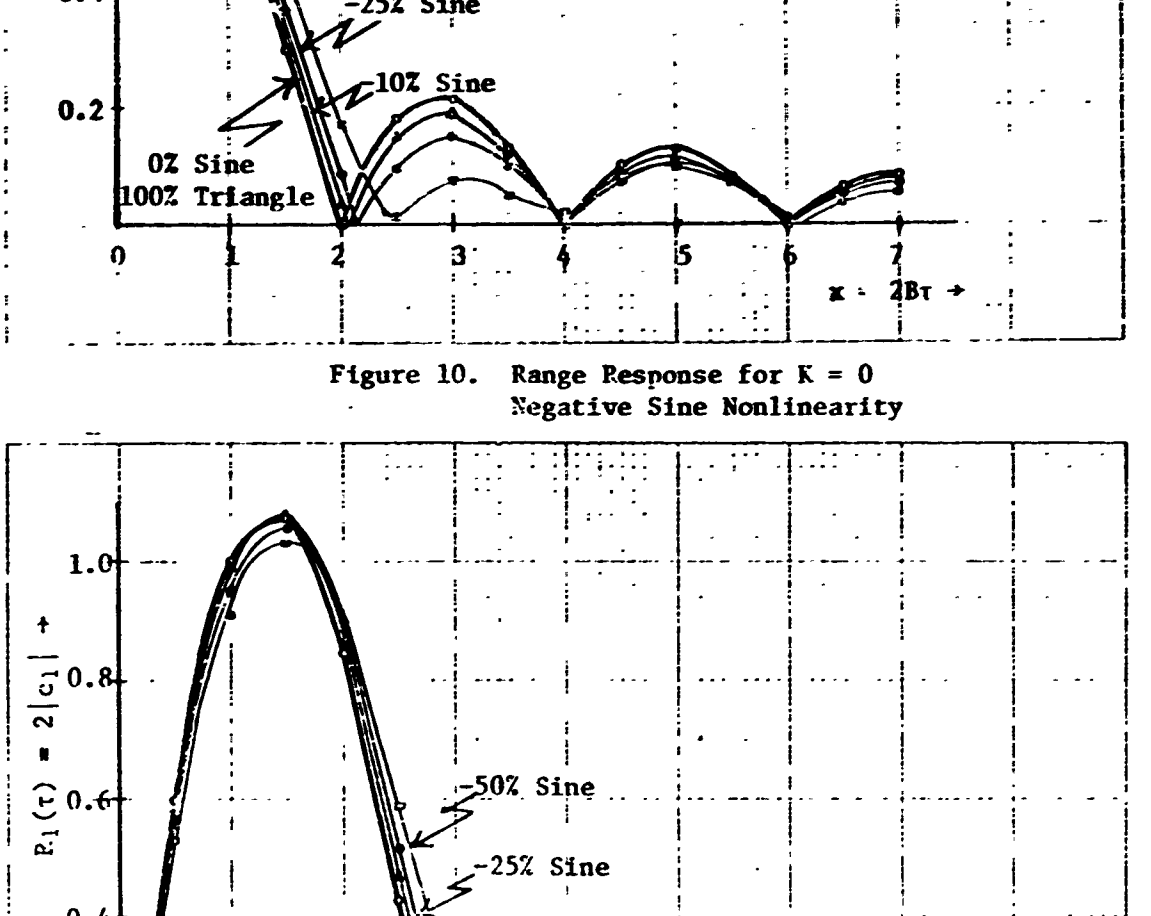

Figure 11. Range Response for K = 1
Negative Sine Nonlinearity

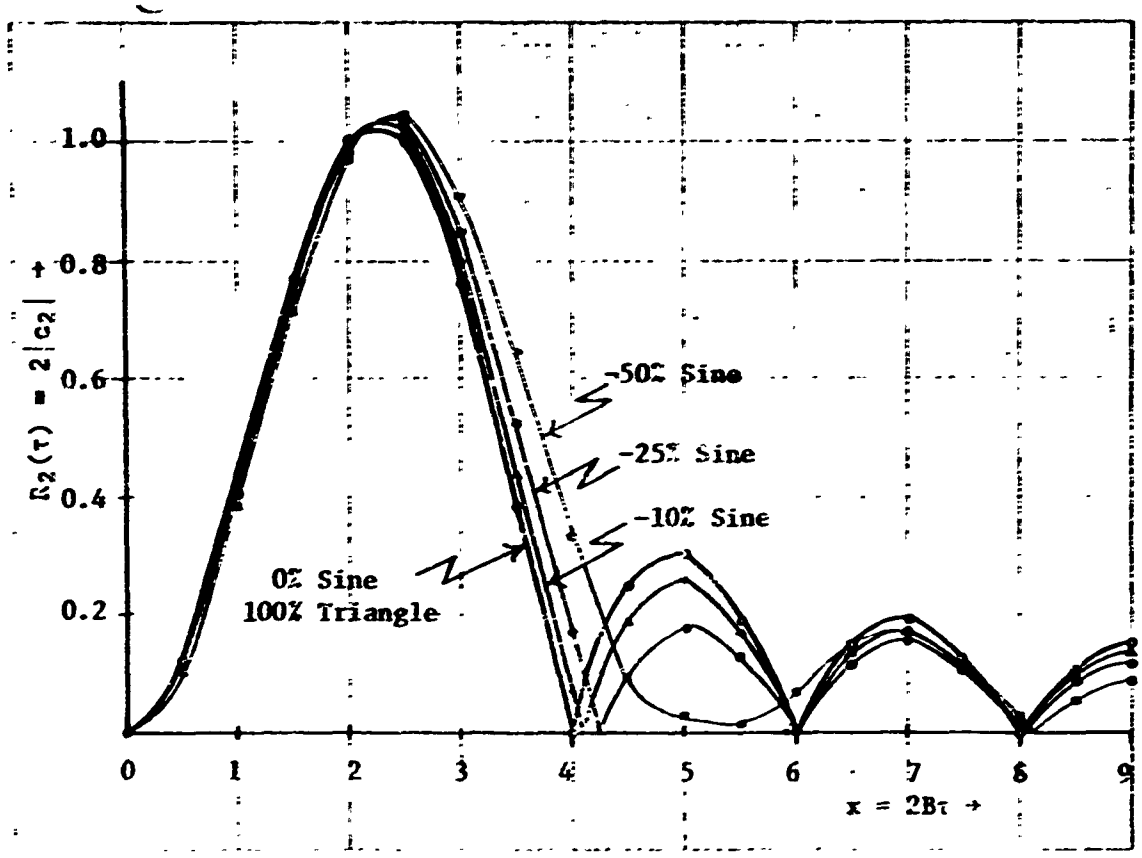

Figure 12. Range Response for K = 2
Negative Sine Nonlinearity

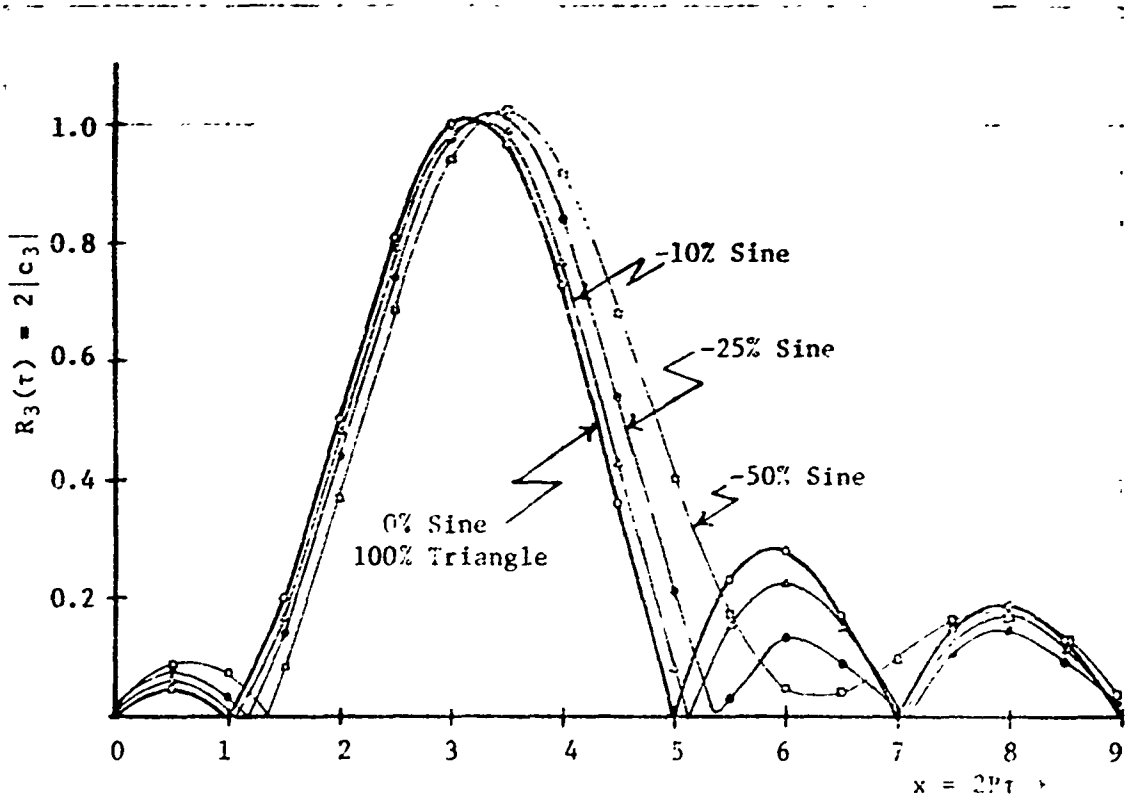

Figure 13. Range Response for K = 3
Negative Sine Nonlinearity

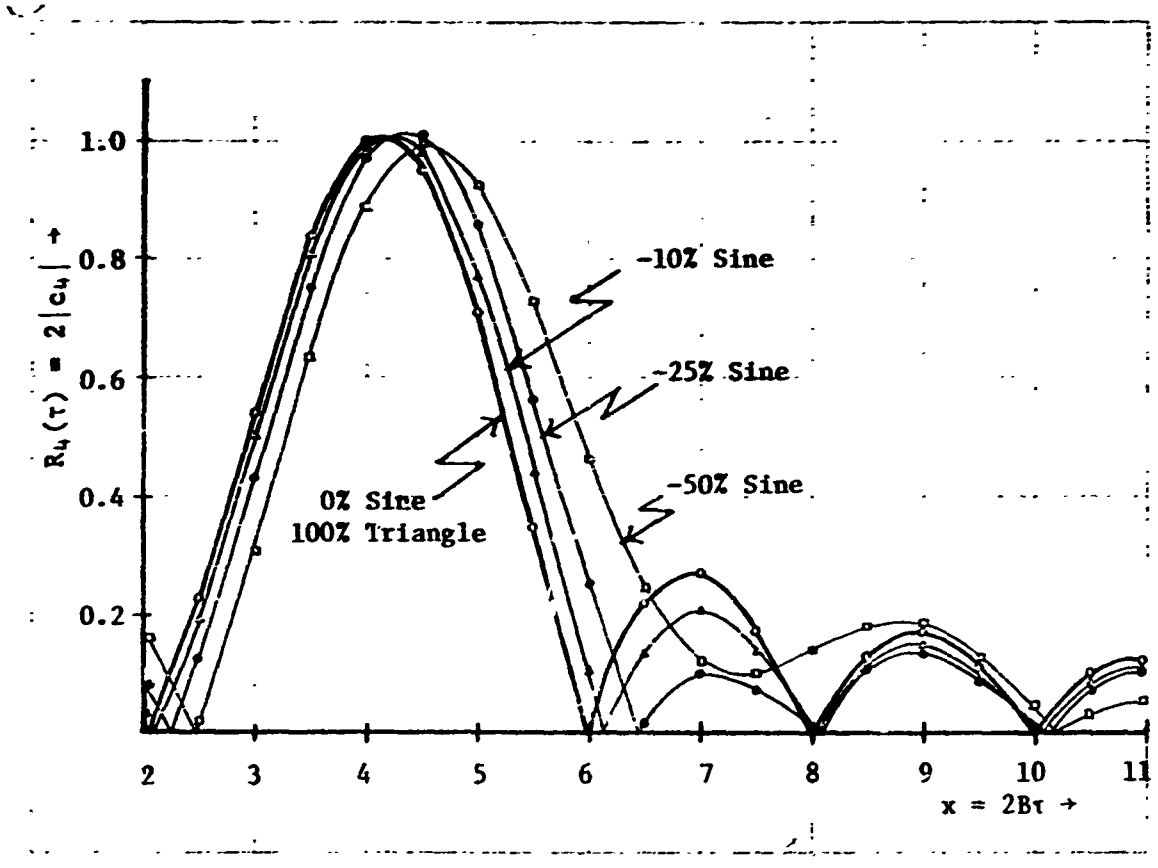

Figure 14. Range Response for K = 4
Negative Sine Nonlinearity

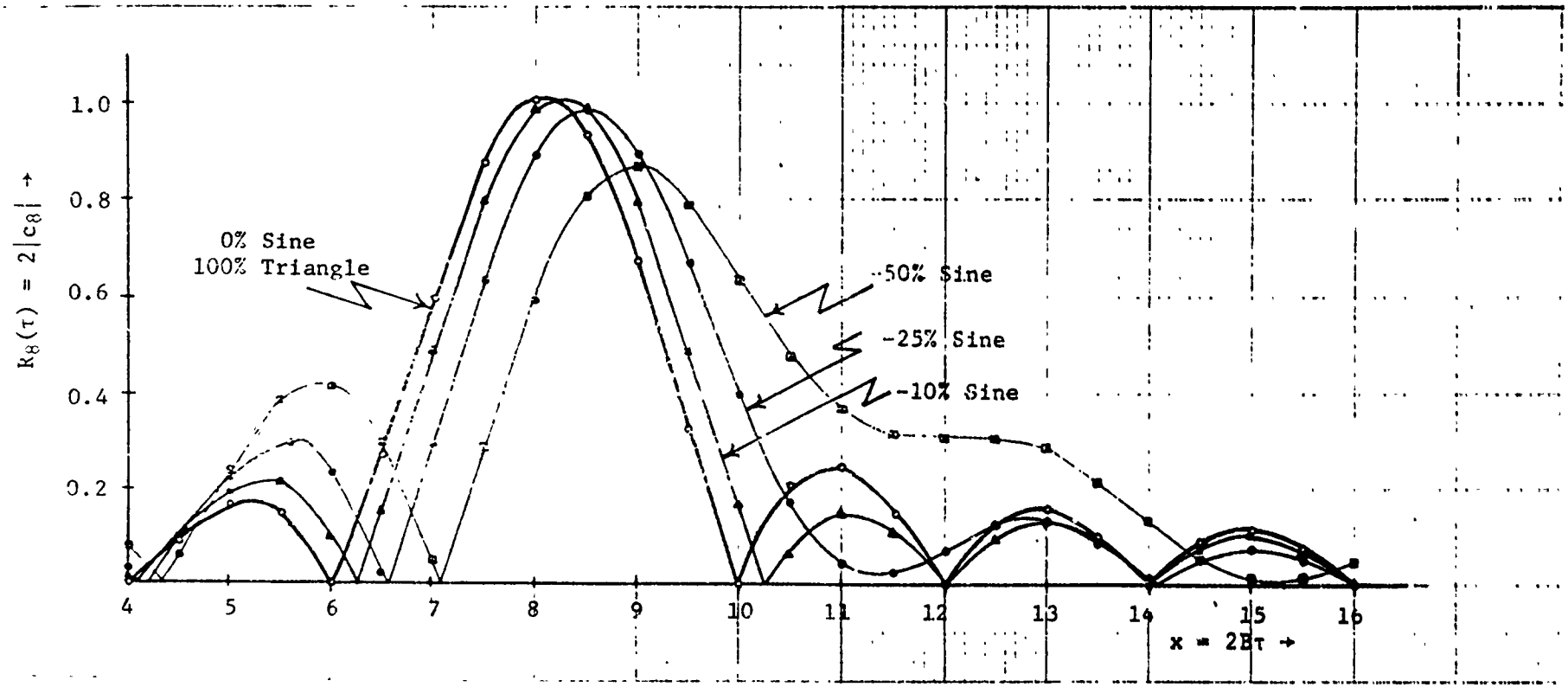

Figure 15. Range Response for K = 8
Negative Sine Nonlinearity

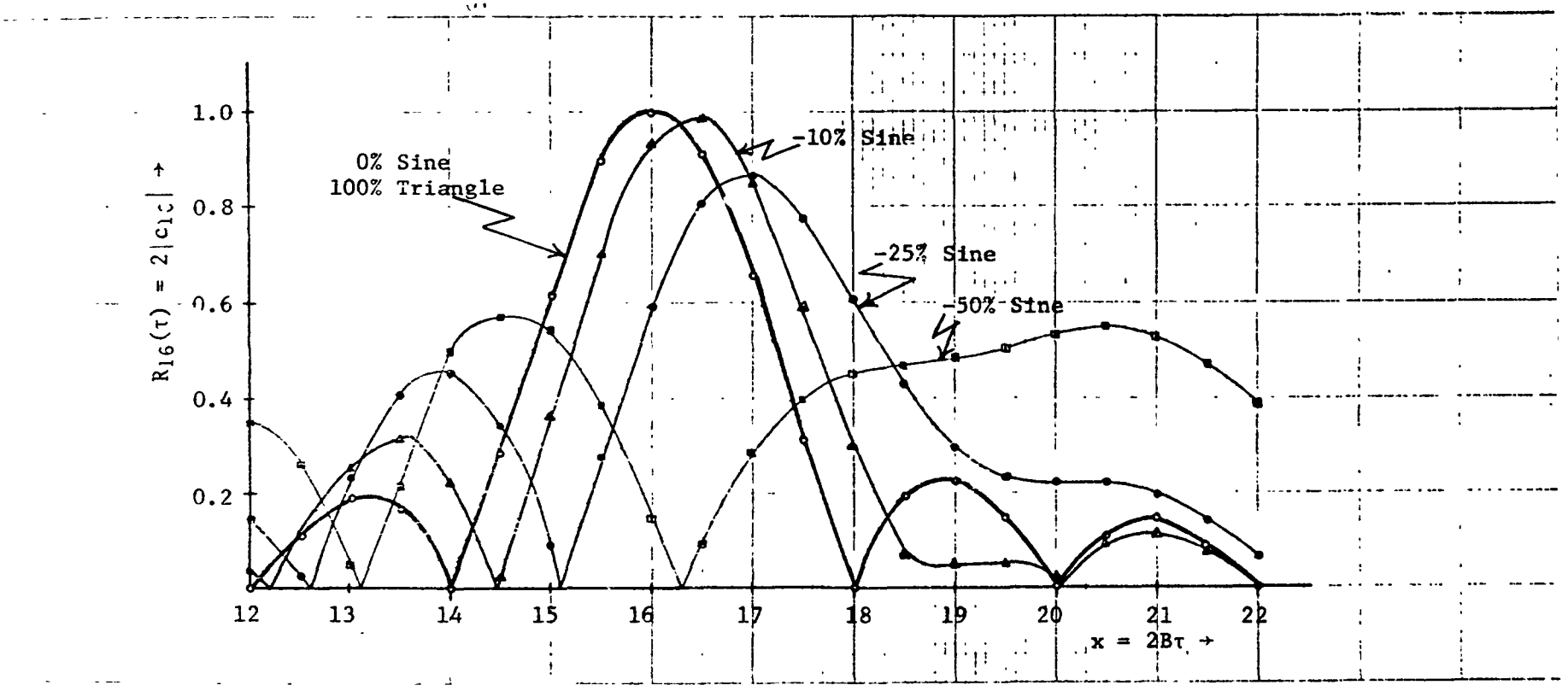

Figure 16. Range Response for N = 16
Negative Sine Nonlinearity

4. RANGE LAW FOR TRIANGLE PLUS CUBE-LAW NONLINEARITY

The range laws, $k_k(\tau)$, will now be evaluated assuming periodic modulation by a composite waveform which is the sum of a pure triangle plus a cube-law as shown in Figure 17 below.

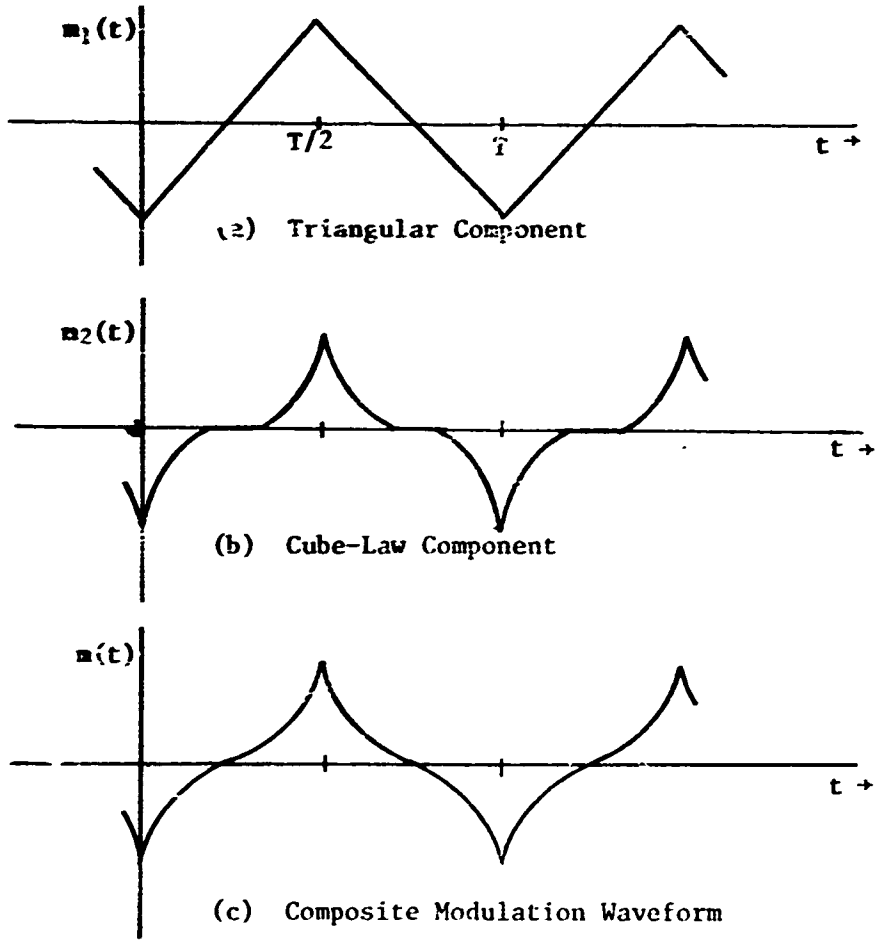

Figure 17. Triangle Plus Cube-Law Nonlinearity

The composite waveform is described by

$$m(t) = m_1(t) + m_2(t) \tag{27}$$

where

$$m_1(t) = \begin{cases} c(t - T/4) & , \quad 0 \le t \le T/2 \\ -c(t - (3/4)T) & , \quad T/2 \le t \le T \end{cases} \tag{28}$$

and

$$m_2(t) = \begin{cases} d(t - T/4)^3 & , \quad 0 \le t \le T/2 \\ -d(t - (3/4)T)^3 & , \quad T/2 \le t \le T \end{cases} \tag{29}$$

c and d are constants to be determined by the percentage of cube-law nonlinearity.

Just as in Section 3, the amount of cube-law nonlinearity added to the triangular component is defined by the percentage of cube-law contribution to the composite peak value measured at the time that the peak value occurs. Thus, the percent cube-law nonlinearity is given by $100P_c$ where

$$P_c \triangleq \frac{d(T/4)^3}{d(T/4)^3 + c(T/4)} = \frac{d(T/4)^2}{d(T/4)^2 + c} \quad . \tag{30}$$

The range laws resulting from this triangle plus cube-law nonlinearity are described by (see Appendix C for the derivation)

$$R_k(\tau) = \begin{cases} |c_0(\tau)| & , \quad k = 0 \\ 2|c_k(\tau)| & , \quad k = 1,2 \ldots \end{cases} \tag{31}$$

where

$$c_k(\tau) = \frac{1}{\pi} \int_0^{\pi} e^{j\{P_t\theta + P_c(2/\pi)^2[(\theta-\pi/2)^3 + (\pi/2)^3]\}x} \cos(k\theta)d\theta \tag{32}$$

$$x \triangleq 2B \tag{33}$$

$$P_t \triangleq 1 - P_c \tag{34}$$

and B is the peak-to-peak frequency deviation (Hz) of the composite frequency modulating waveform. For $B >> f_m$, which is usually the case, B corresponds to the spectral bandwidth (Hz) of the transmitted RF signal.

For the case of $P_c = 0$, i.e. pure triangular modulation, (32) reduces to our well-known sin z/z type result given by (24).

Once again the percentage of modulation may be positive or negative depending on the sign of d with respect to c in (30). By comparing the shapes of the sinusoidal and cube-law modulating waveforms (see Figure 2 and 17) it is seen that the shape obtained for a positive cube-law nonlinearity is roughly equivalent to that obtained using a negative sinusoidal nonlinearity. (The exact relationship is discussed in Section 5.2). Thus, in comparing the results

for cube-law nonlinearity with those for sinusoidal nonlinearity, we would expect the sidelobe level in the range laws obtained for small percentages of *positive* cube-law nonlinearity to be suppressed with respect with those obtained using pure triangular modulation. The converse is also true. Since only the positive cube-law nonlinearity gives sidelobe suppression while negative cube-law nonlinearity gives increases in the sidelobe levels, only the positive cube-law results will be given here.

The range laws for several positive percentages of cube-law nonlinearity are shown in Figures 18-24. These curves were obtained by evaluating (32) numerically. It is evident that this type of nonlinearity moves the range laws to the right; that is, it increases x_0. Furthermore, if the percent nonlinearity is not too large the sidelobe level is decreased at distances greater than x_0. From these figures, the optimum decrease in sidelobe level is obtained when the (positive) percentage of cube-law nonlinearity is set to approximately

$$P_c \approx 1/k+4 \quad , \tag{35}$$

Thus, some positive cube-law nonlinearity is desirable, and negative cube-law nonlinearity is undesirable.

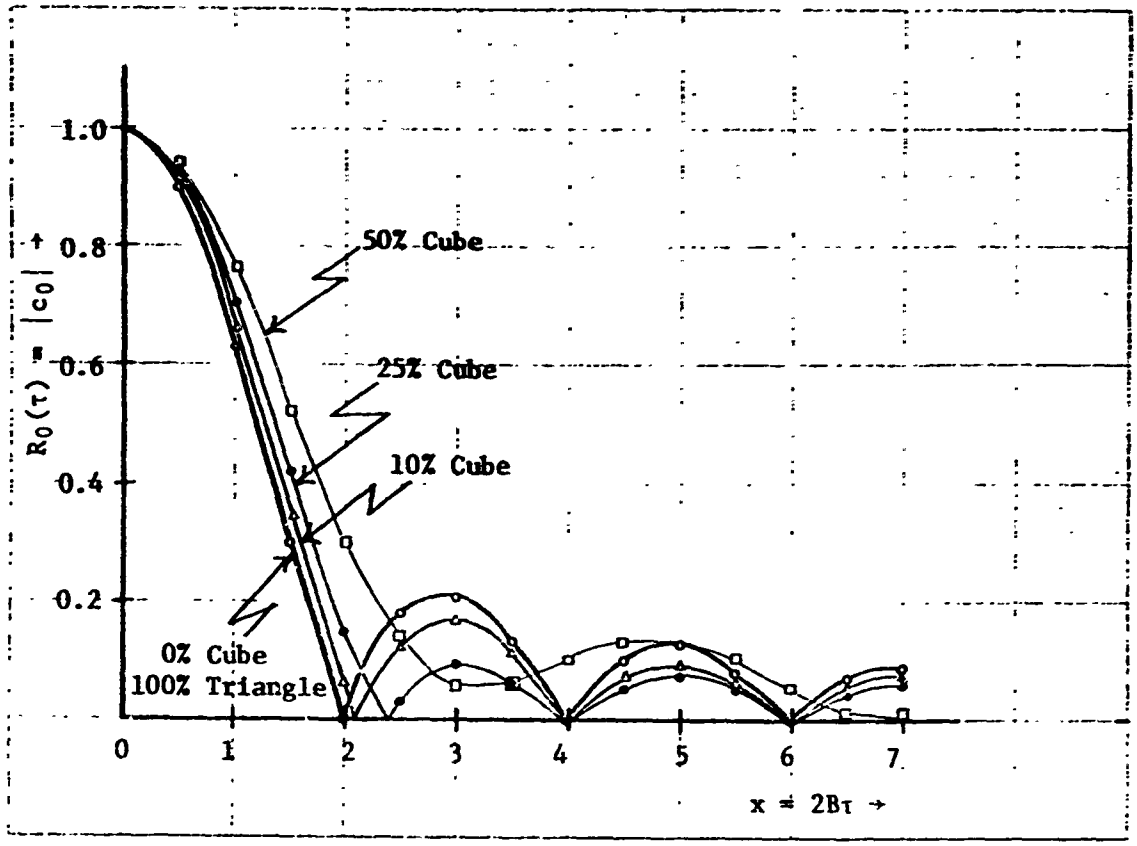

Figure 18. Range Response For K = 0
Cube-Law Nonlinearity

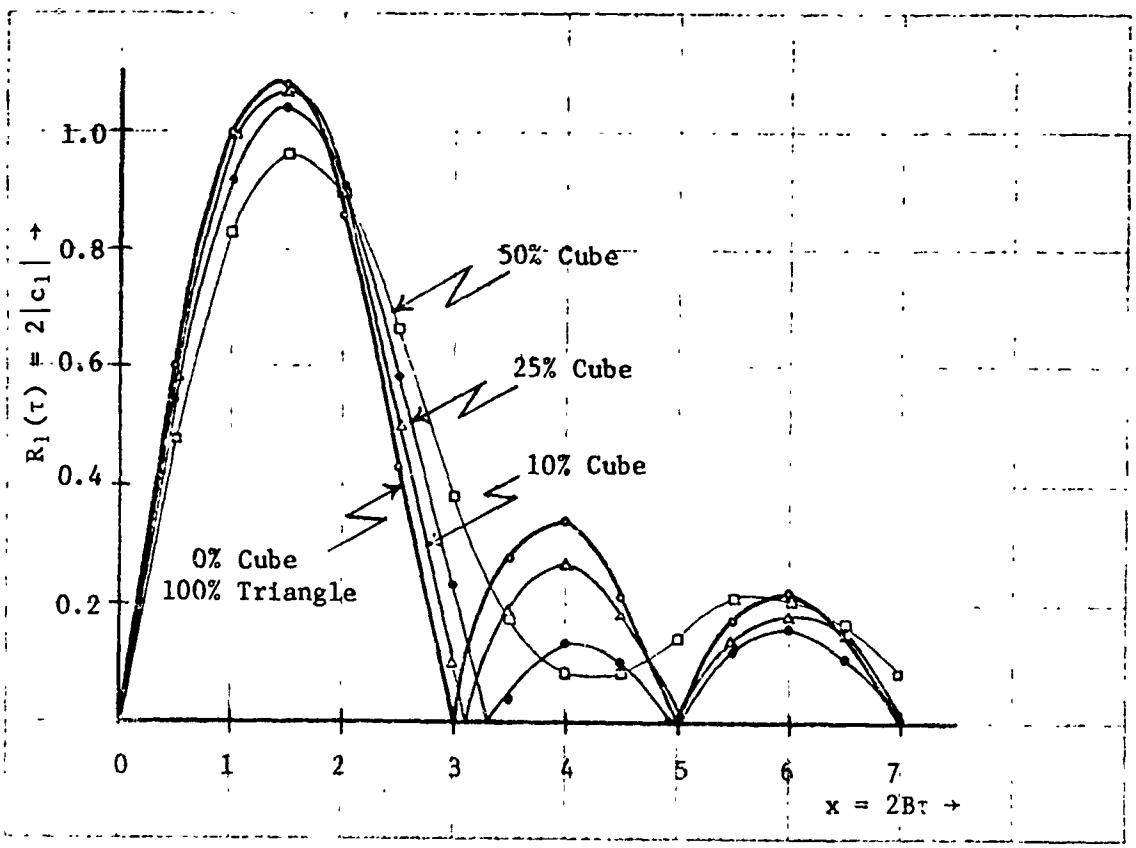

Figure 19. Range Response for K = 1
Cube-Law Nonlinearity

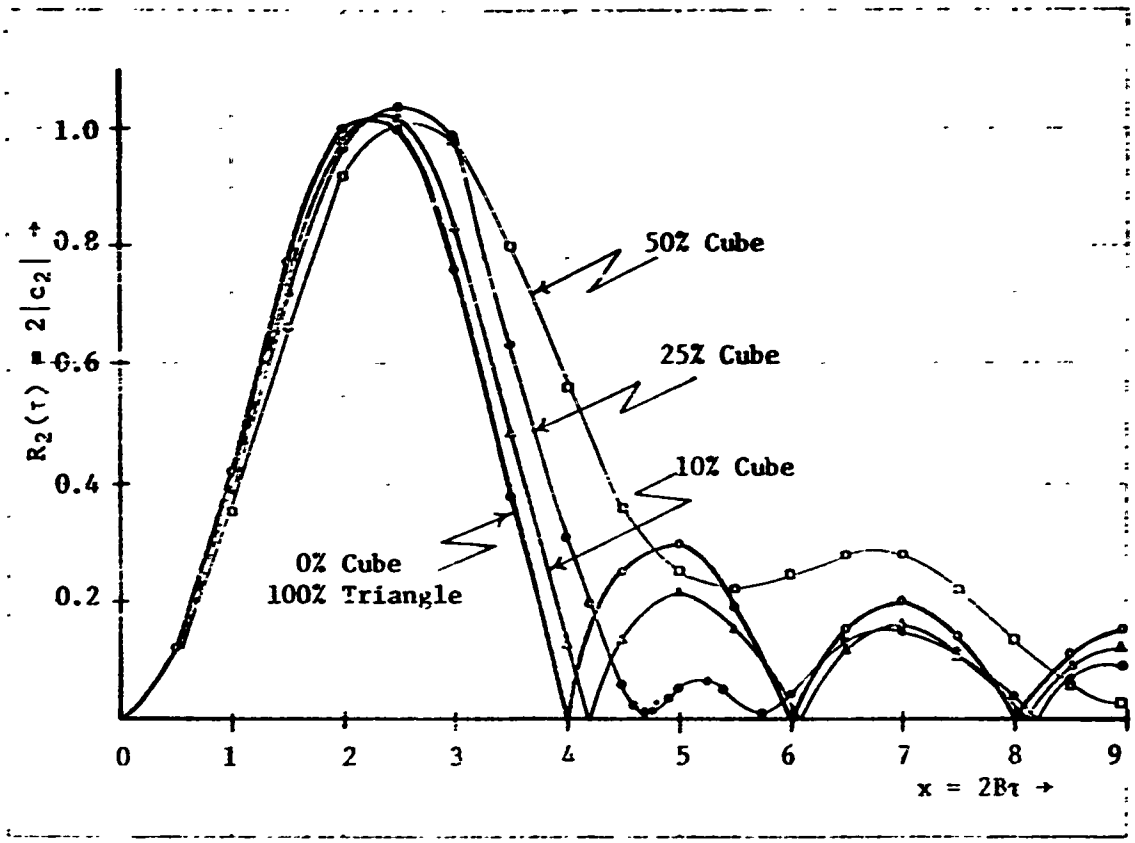

Figure 20. Range Response for K = 2
Cube-Law Nonlinearity

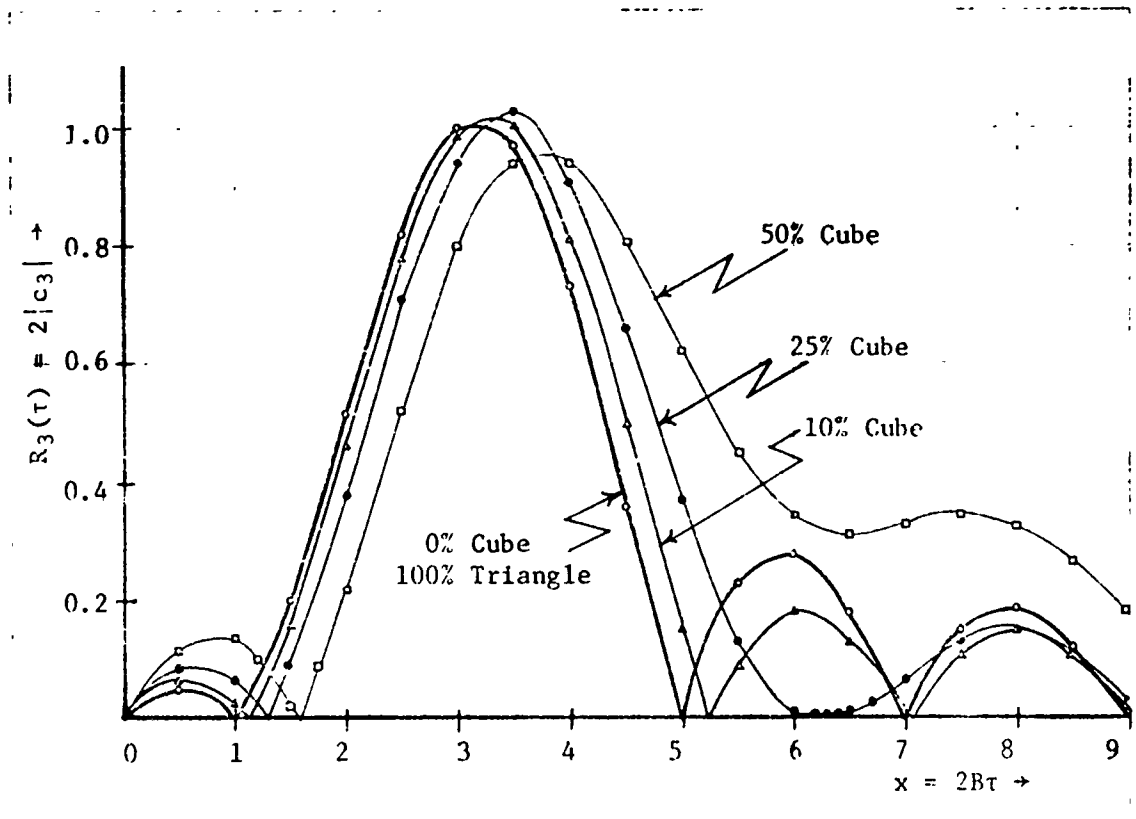

Figure 21. Range Response for K = 3
Cube-Law Nonlinearity

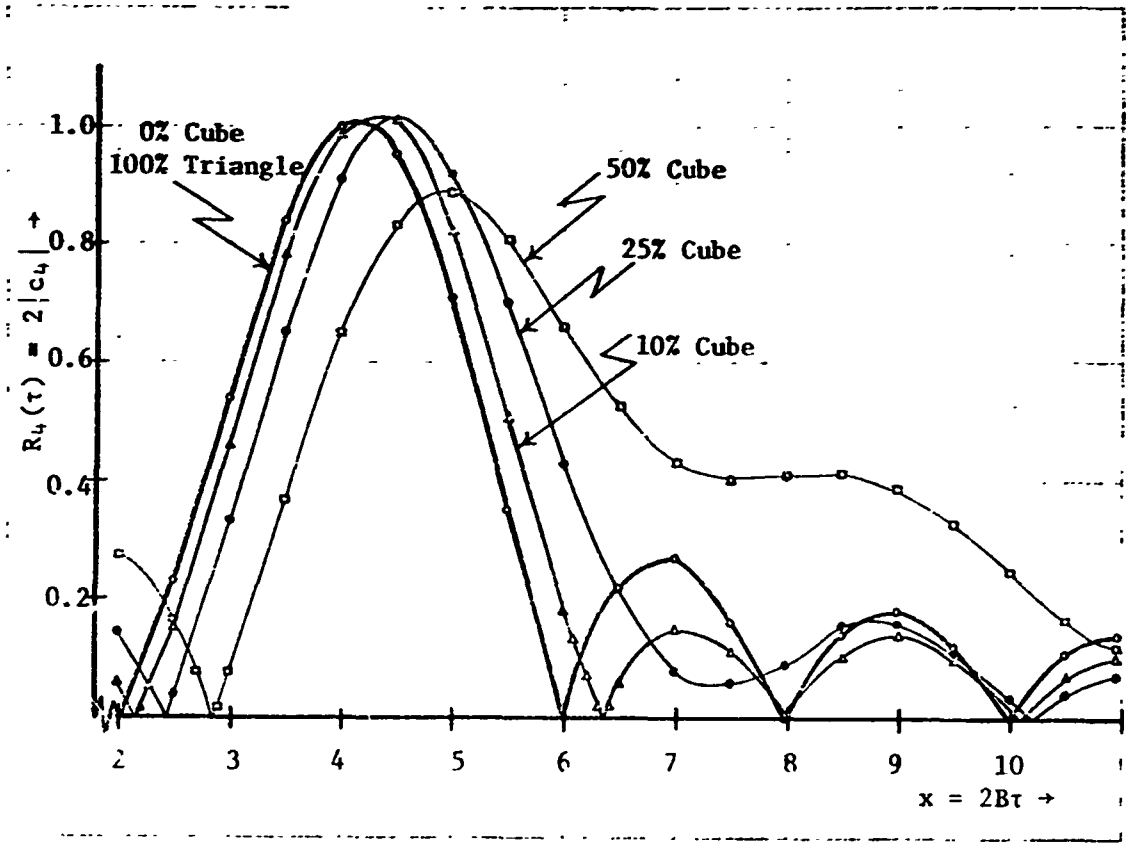

Figure 22. Range Response for K = 4
Cube-Law Nonlinearity

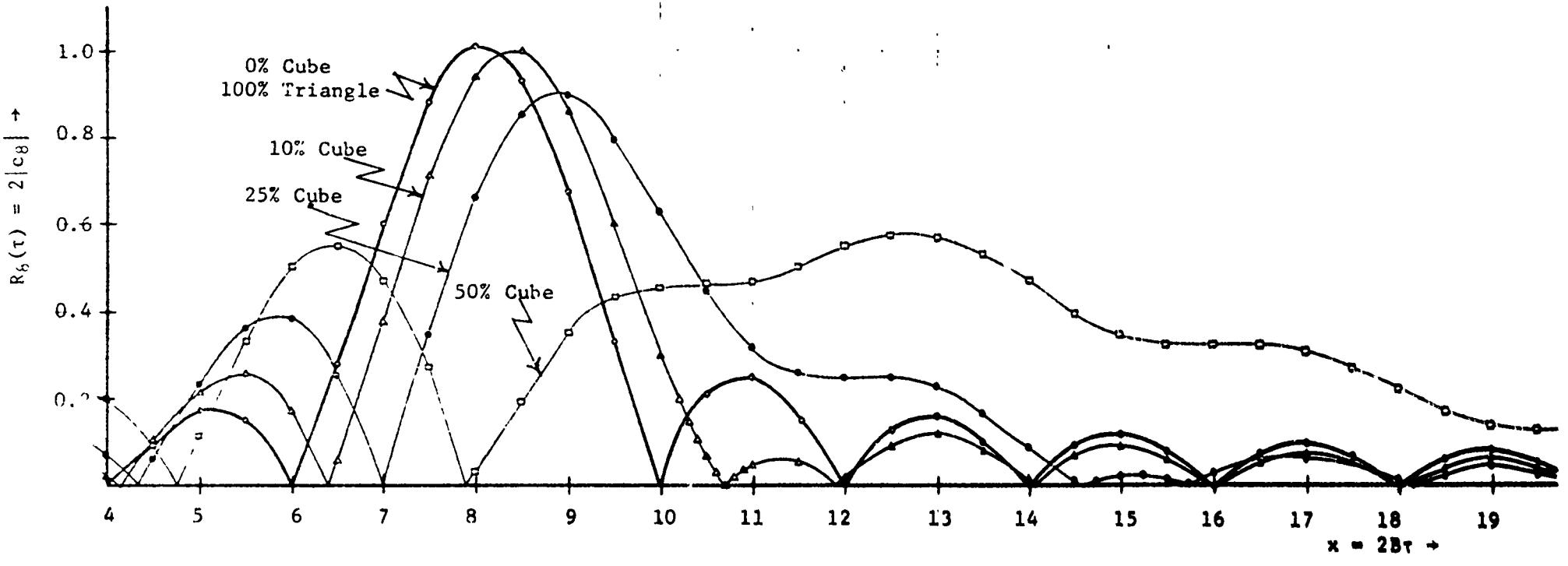

Figure 23. Range Response For K = 8
Cube-Law Nonlinearity

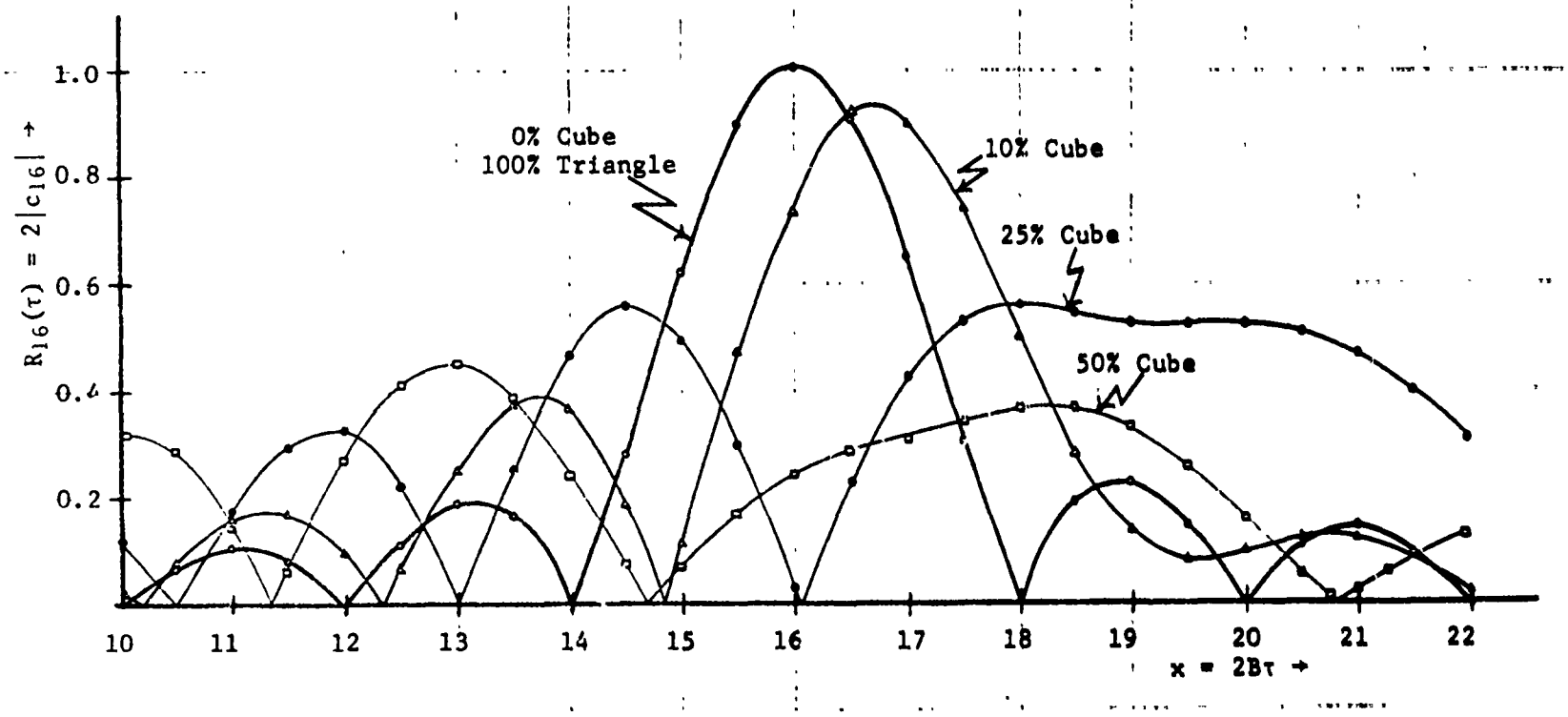

Figure 24. Range Response for K = 16
Cube-Law Nonlinearity

5. EXPERIMENTAL AND THEORETICAL VERIFICATION OF RESULTS

5.1 Experimental Verification

For the case of triangle plus sinusoidal modulation, the two limit results (i.e. pure triangle or pure sinusoidal modulation) are well-known. Since the theoretical range laws given in Figures 3-9 fall within these known limits, these results are already verified experimentally.

For the case of triangle plus cube-law modulation, the theoretical range laws have been given by Figures 18-24. These results will now be verified experimentally by using the test apparatus shown in Figure 25 below. The FM oscillator was supplied by HDL and is capable of large peak-to-peak deviations with little incidental AM. B was set to 20MHz and f_m was 5KHz. The experimental results are shown in Figures 26 and 27.

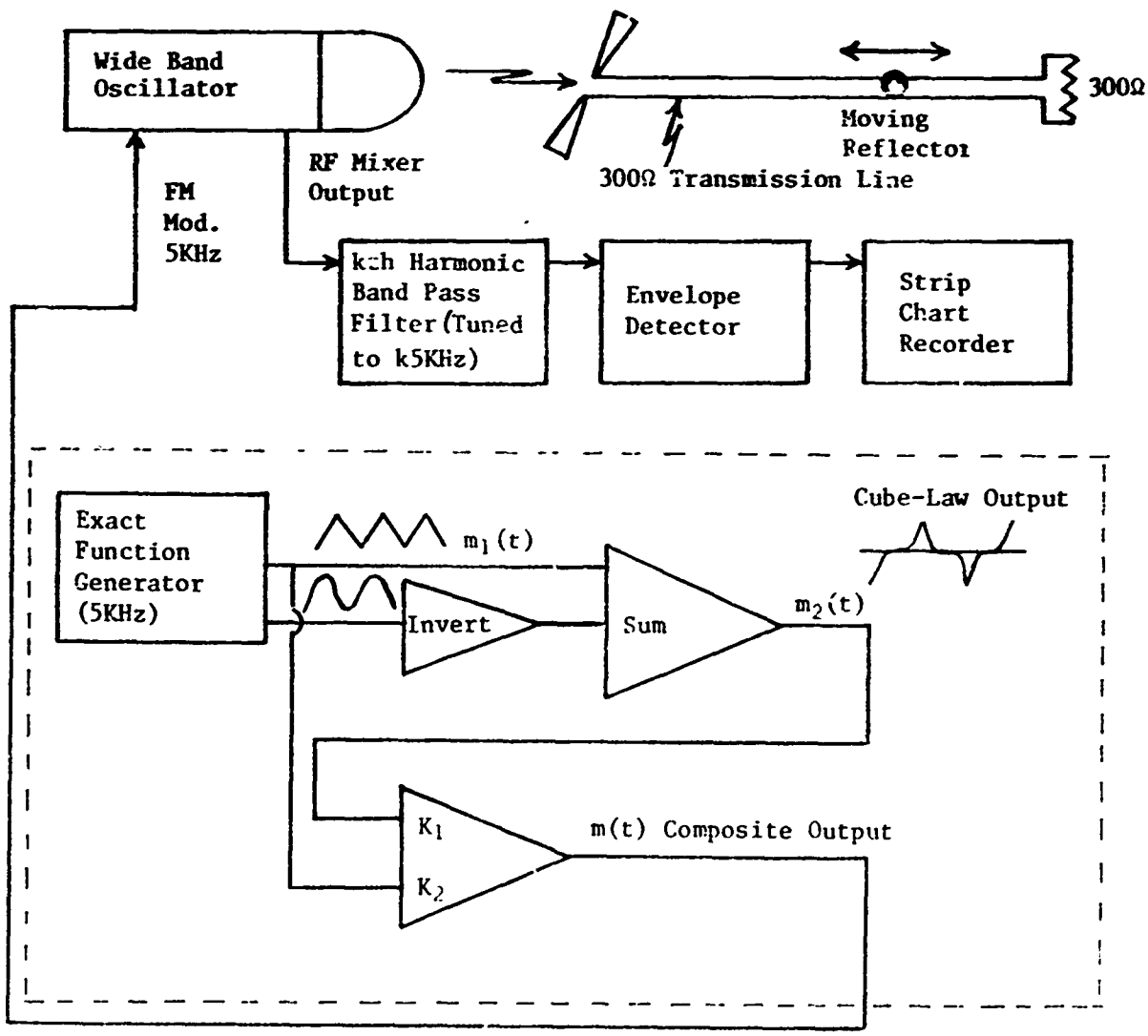

Figure 25. Test Apparatus For Experimental Measurement of Range Laws

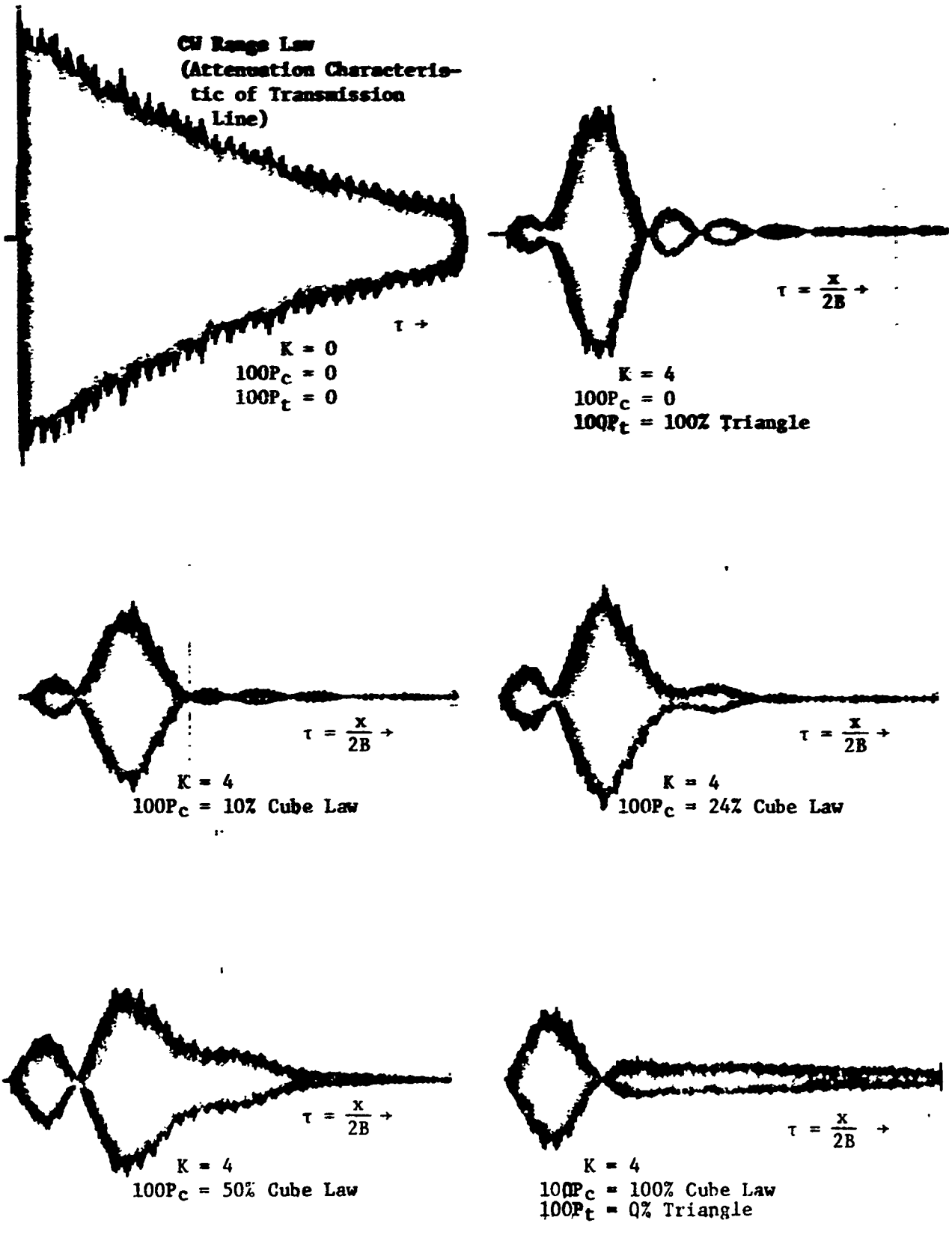

Figure 26. Experimental Range Laws for K = 4--
Triangle Plus Positive Cube-Law Nonlinearity

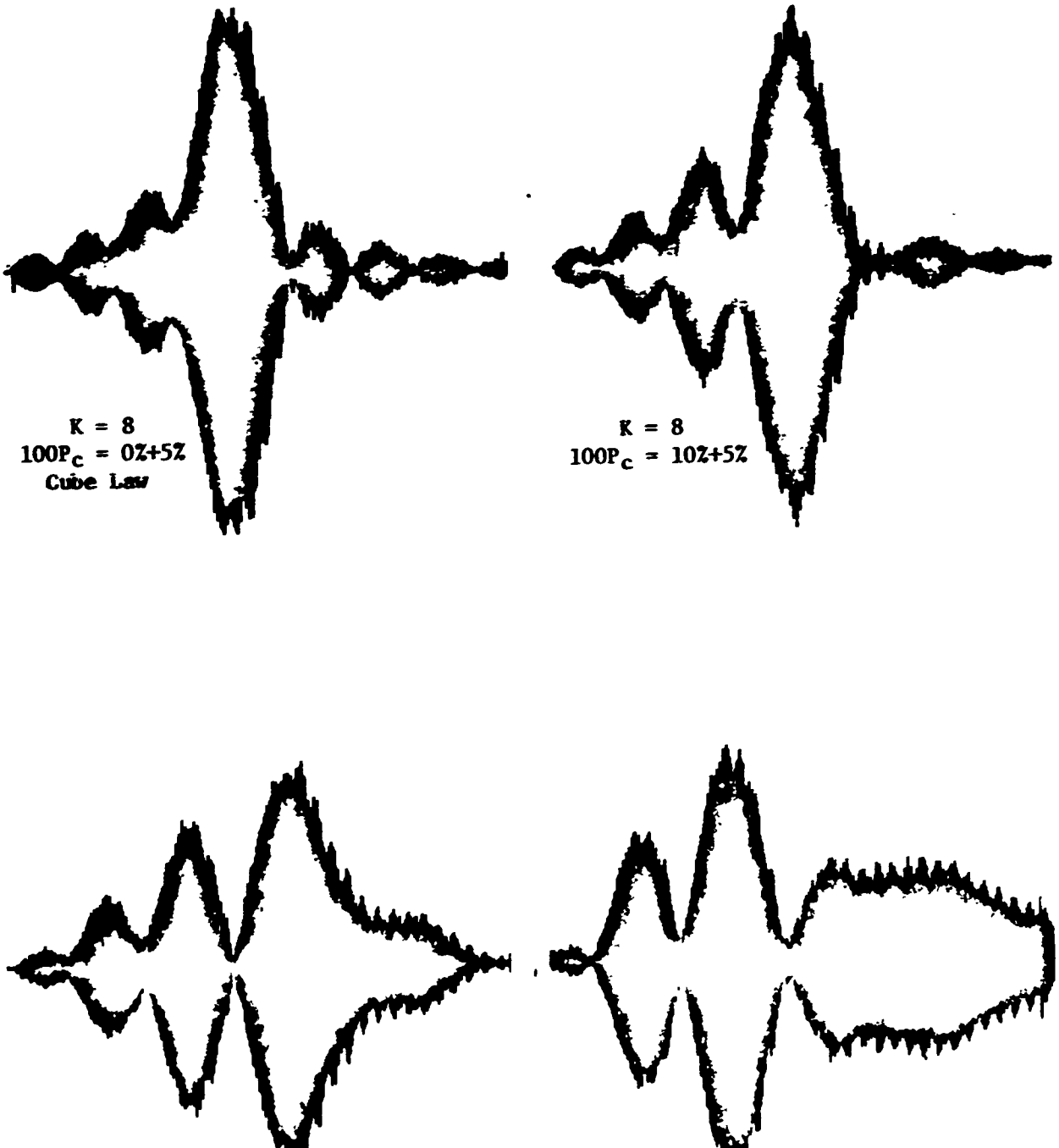

Figure 27. Experimental Range Laws for K = 8--
Triangle Plus Positive Cube-Law Nonlinearity

It is seen that these experimental results agree with Figures 22 and 23 when the attenuation characteristic of the transmission line in the experimental apparatus is taken into account.

5.2 Theoretical Verification

If negative percentages of cube-law modulation are used we have a modulating waveform of the form

$$m(t) = k_1 t - k_2 t^3 \quad , \quad -T/4 \leq t \leq T/4 \tag{36}$$

where the $t = 0$ axis has been shifted by $T/4$ for analytical simplification. This may be compared with the waveform shape that is obtained for triangle plus sinusoidal nonlinearity

$$m(t) = k_3 t - k_4 t^3 + \text{higher order terms} \tag{37}$$

where the expansion $\sin\theta = \theta - (1/3!)\theta^3 + (1/5!)\theta^5 \ldots$ has been used (see Appendix D). Neglecting the terms of order higher than t^3, a relationship between the percentage of cube-law nonlinearity and the percentage of sinusoidal nonlinearity can be obtained such that the two waveforms of (36) and (37) are equivalent; that is $k_1 = k_2$ and $k_2 = k_4$. Referring to Appendix D, the result is

$$P_c = \frac{-\dfrac{1}{6(2/\pi)^3} P_s}{1 - \dfrac{P_s}{\dfrac{6(2/\pi)^3}{6(2/\pi)^2(1-2/\pi)-1}}} = \frac{-0.64596 P_s}{1 - \dfrac{P_s}{13.304}} \tag{38}$$

which may be approximated by

$$P_c \approx -0.646 P_s \tag{39}$$

when $|P_s| < 1$. Equation (39) is plotted in Figure 28.

Using (38), some range laws for cube-law nonlinearity which are equivalent to the sinusoidal nonlinearity are shown in Figure 29. It is seen that Figure 29 is almost identical to Figure 4. Thus, the theoretical results for the cases of cube-law and sinusoidal nonlinearity are verified theoretically with respect to each other.

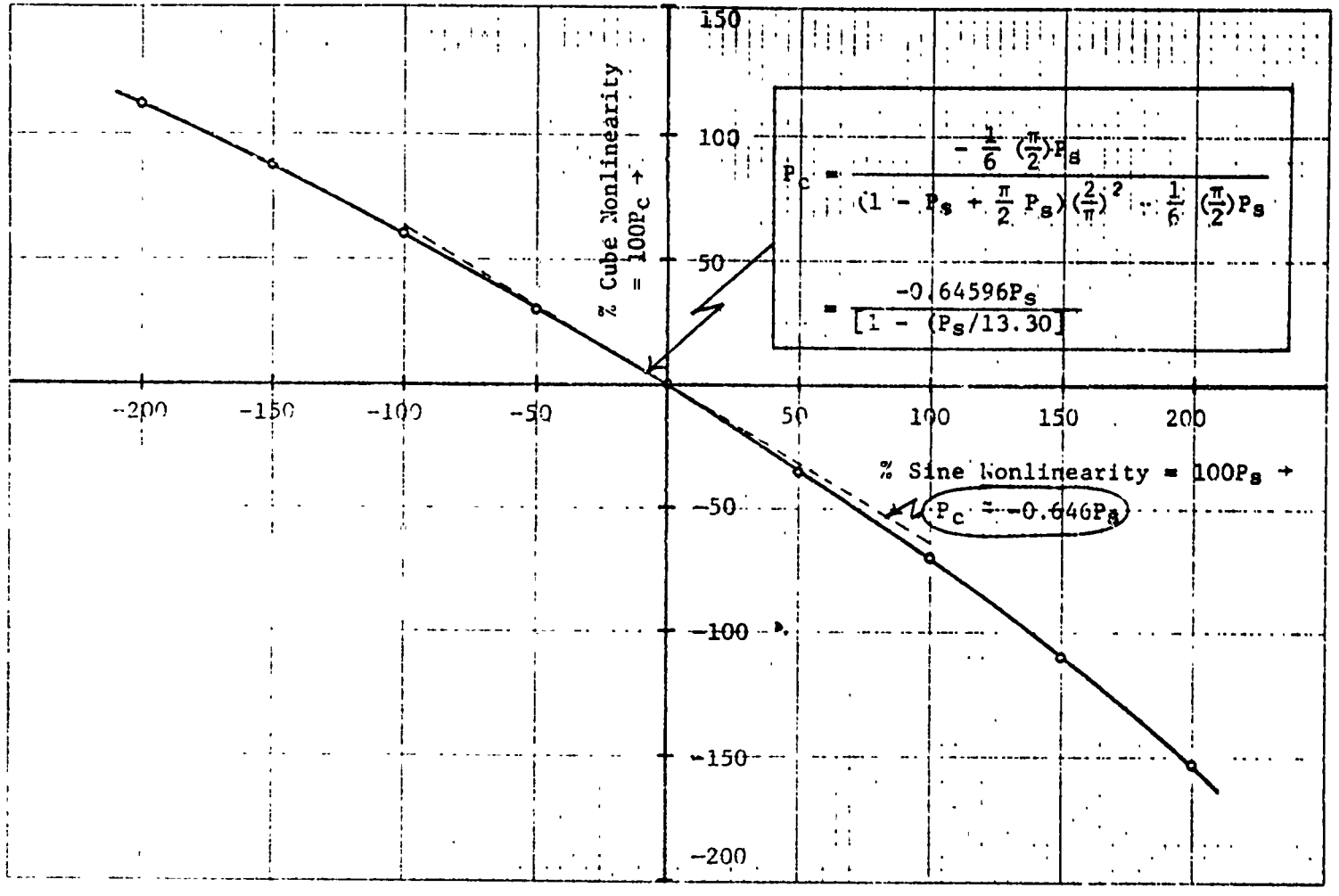

Figure 28. P_C vs P_S For Approximately Equivalent Cube-Law and Sinusoidal Nonlinearities

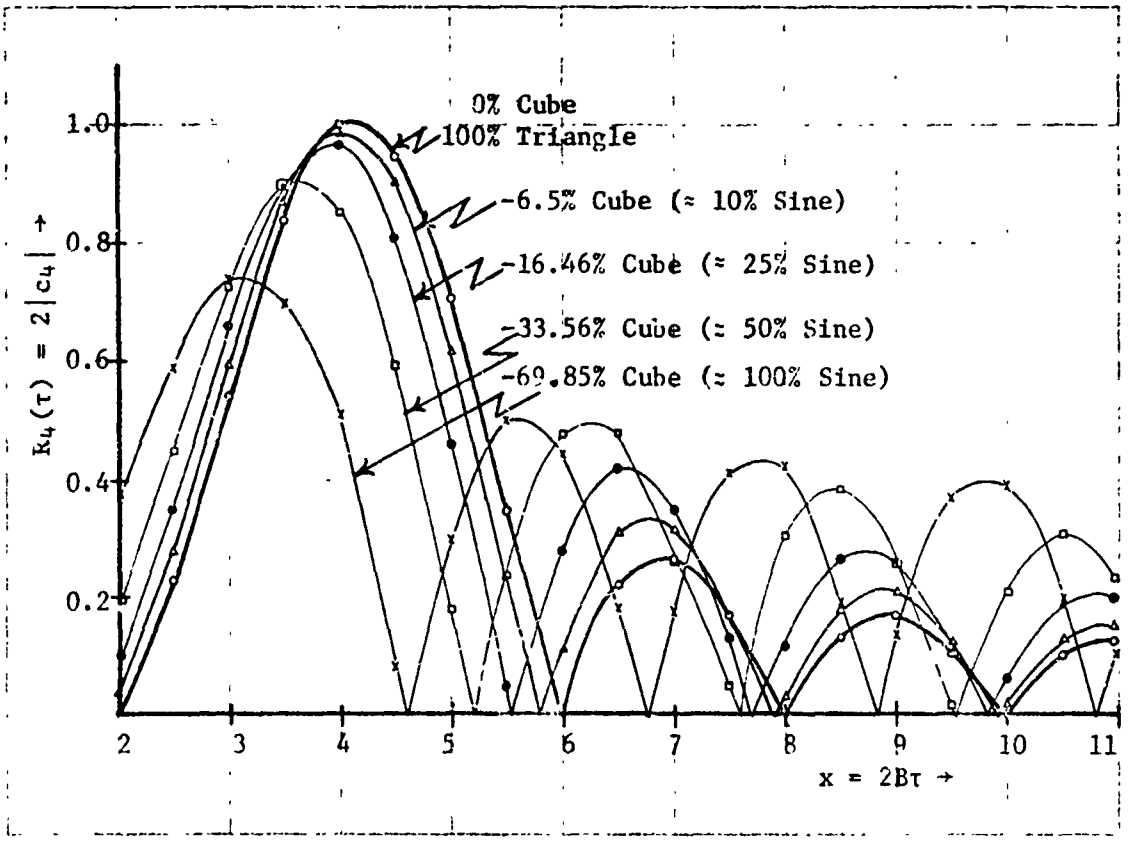

Figure 29. Comparison of Range Laws--
Cube-Law Nonlinearity, K=4

6. SUMMARY

Range laws have been obtained for a class of distance measuring systems. This class radiates an RF signal which is frequency modulated by a nonlinear triangular waveform. The nonlinearity consists of one of two shapes--Type I and Type II--as shown in Figure 30. Type I nonlinearity may be synthesized from a triangle plus a positive sinusoidal nonlinearity or from a triangle plus a negative cube-law nonlinearity. Type II may be synthesized from a triangle plus a negative sinusoidal nonlinearity or a triangle plus a positive cube-law nonlinearity.

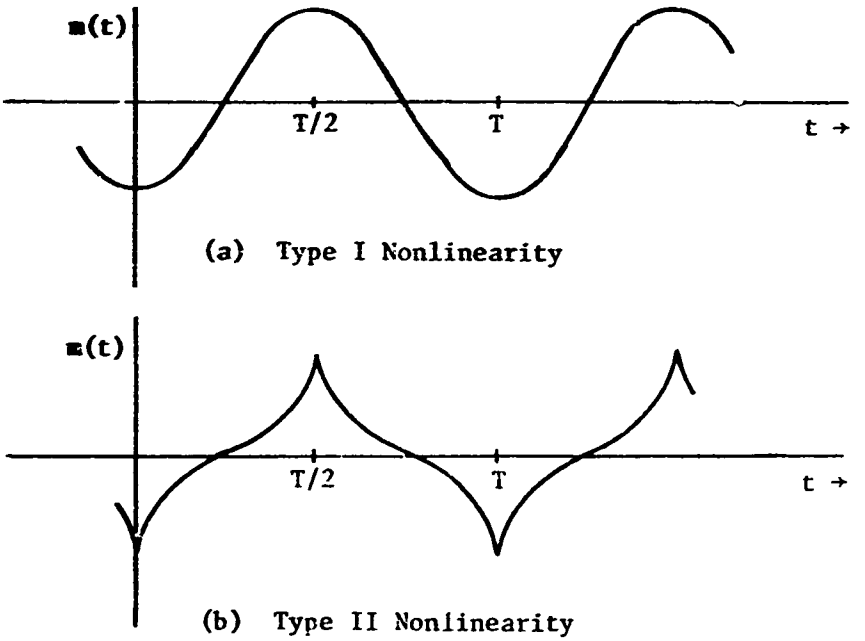

Figure 30. Nonlinear Frequency Modulating Waveforms

The amount of nonlinearity is specified by a parameter which gives the percentage contribution of the sinusoidal ($100P_S$) or cube-law ($100P_C$) nonlinearity with respect to the composite waveform amplitude at the time when the peak value occurs (i.e. t = 0, T/2, T, etc.). These percentages may have positive or negative values.

The resulting range laws show that the nonlinearity may be desirable or undesirable. The Type I nonlinearity produces an undesirable effect (Figures 3-9) since the sidelobe levels are increased over those obtained for pure triangular modulation, for all distances greater than x_0. The Type II nonlinearity produces a desirable effect (Figures 11-16 and 18-24) provided that the percentage of nonlinearity is not too large. That is, the sidelobe levels are decreased for distances greater than x_0 if P_S or P_C is small and of the correct

sign. From the figures it is seen that a sinusoidal nonlinearity with

$$P_s \approx -1.5\ (1/k+4) \tag{40}$$

or a cube-law nonlinearity with

$$P_c \approx 1/(k+4) \tag{41}$$

gives the optimum sidelobe suppression and that the x_0 is not shifted very much for these small percentages of nonlinearity.

In summary, the results of this report may be used to evaluate existing distance measuring systems and to design new systems. The range laws of existing systems may be predicted for the case of frequency modulation by a nonlinear triangular waveform. For new systems, modulating nonlinear triangular waveforms may be prescribed which produce range laws with better sidelobe suppression than those obtained by use of the pure triangular waveform.

APPENDIX A

Fourier Series for the Mixer Output

Equation (9) will now be derived from (3), (7) and (8). The mixer output is

$$y(t,\tau) = \text{Re}\left\{\sum c_k\, e^{jk\omega_m t}\, e^{j\omega_c t}\right\} \quad . \tag{A-1}$$

Expanding $\tau(t)$ in a Taylor's series about t we have

$$\tau(t_0 + t) = \tau(t_0) + \left.\frac{d\tau}{dt}\right|_{t_0} t + \ldots \quad . \tag{A-2}$$

Now

$$\left.\frac{d\tau}{dt}\right|_{t_0} = \frac{\Delta\tau}{\Delta t} = \frac{(2v_r/\Delta s)}{(c/\Delta s)} = \frac{2v_r}{c}$$

where $\Delta\tau$ is the incremental change in the round trip time delay during the incremental time Δt

Δs is the incremental change in distance

v_r is the radial velocity of the target with respect to the DMS

and c is the speed of light.

From (A-2), using the first two terms of the Taylor's series

$$\omega_c\tau = \phi_0 + \omega_d t \tag{A-3}$$

where

$$\phi_0 = \omega_c\tau(t_0)$$

and

$$\omega_d = (2v_r/c)\omega_c \quad .$$

ω_d is the radian doppler frequency. Using (A-3), but neglecting the phase angle ϕ_0, (A-1) becomes

$$y(t,\tau) = \sum_{k=-}^{\infty} \text{Re}\left\{c_k e^{j(k\omega_m + \omega_d)t}\right\}$$

$$= \text{Re}\left[c_0 e^{j\omega_d t}\right] + \sum_{k=1}^{\infty} \text{Re}\left\{\left[c_k e^{jk\omega_m t} + c_{-k} e^{-jk\omega_m t}\right] e^{j\omega_d t}\right\} \quad . \tag{A-4}$$

We will now show that $c_k = c_{-k}$ for the case when the instantaneous difference frequency has odd symmetry; that is when

$$\omega_{id}(t,\tau) = -\omega_{id}(-t,\tau) \tag{A-5}$$

From (8)

$$c_k = \frac{1}{T} \int_0^T e^{j\theta_d(t,\tau)}\, e^{-jk\omega_m t}\, dt \tag{A-6}$$

and

$$c_{-k} = \frac{1}{T} \int_0^T e^{j\theta_d(t,\tau)}\, e^{jk\omega_m t}\, dt \quad . \tag{A-7}$$

Letting $\sigma = -(t + T)$, (A-7) becomes

$$c_{-k} = \frac{1}{T} \int_0^T e^{j\theta_d[(T-\sigma),\tau]}\, e^{-jk\omega_m \sigma}\, d\sigma \ . \tag{A-8}$$

Identifying (A-8) with (A-6) we see that a sufficient requirement for $c_{-k} = c_k$ is that

$$\theta_d[t,\tau] = \theta_d[(T-t),\tau]$$

and since θ_d is periodic with period T, this is equivalent to the requirement

$$\theta_d[t,\tau] = \theta_d[-t,\tau] \tag{A-9}$$

Taking the derivative of both sides of (A-9)

$$\omega_{id}(t,\tau) = \frac{d\theta(t,\tau)}{dt} = \frac{-d\theta_d(x,\tau)}{dx}\bigg|_{x=-t} = -\omega_{id}(-t,\tau)$$

Thus

$$c_k = c_{-k} \text{ if } \omega_{id}(t,\tau) = -\omega_{id}(-t,\tau) \tag{A-10}$$

Using (A-10) in (A-4) we have

$$y(t,\tau) = |c_0| + \sum_{k=1}^{\infty} 2|c_k| \cos\left[\omega_d t + \angle c_k\right] \cos\left(k\omega_m t\right) \tag{A-11}$$

provided that $\omega_{id}(t,\tau) = -\omega_d(-t,\tau)$

where $|[\cdot]|$ denotes the magnitude of $[\cdot]$

and $\angle[\cdot]$ denotes the angle of $[\cdot]$.

Now let t_0 be defined as the value of t which gives the first turn-around of the modulation, m(t). This is illustrated in the figure below for the case of m(t) having a triangular waveshape.

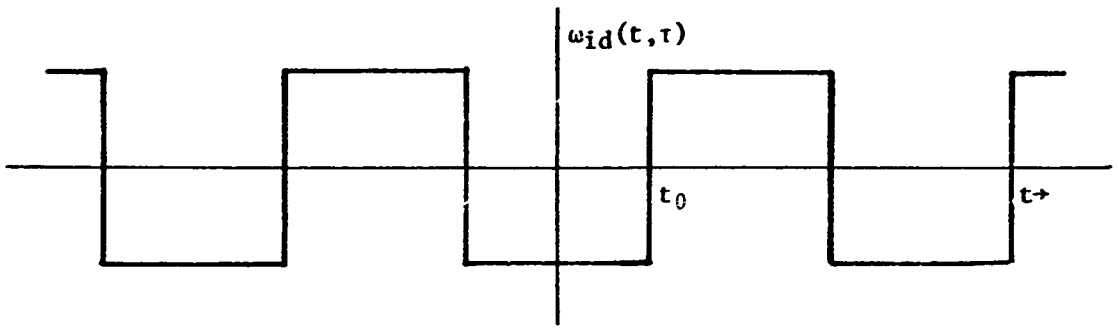

Then, using the above sufficient condition for $c_k = c_{-k}$, we have the requirement, from (A-5), that

$$\omega_{id}[(t-t_0),\tau] = -\omega_{id}[-(t-t_0),\tau] \qquad \text{(A-12)}$$

and (A-11) becomes

$$y(t,\tau) = |C_0| + \sum_{k=1}^{\infty} 2|c_k| \cos[\omega_d(t-t_0) + c_k] \cos[k\omega_m(t-t_0)] \qquad \text{(A-13)}$$

Furthermore, since ω_{id} is periodic with period T, (A-12) is satisfied if we require the difference frequency to have half-wave odd symmetry, that is if

$$\omega_{id}(t,\tau) = -\omega_{id}(t + \frac{T}{2}, \tau) \quad . \qquad \text{(A-14)}$$

APPENDIX B

Fourier Coefficients For Triangle Plus Sinusoidal Modulation

Using (6), (16) and (17), the difference phase is

$$\theta_d(t,\tau) = \begin{cases} (Da\tau)t + \frac{Db}{\omega_m}\left[\sin\omega_m(t-\tau) + \sin\omega_m\tau - \sin\omega_m t\right] & , \quad 0 \le t \le \frac{T}{2} \\ (-Da\tau)(t-T) + \frac{Db}{\omega_m}\left[\sin\omega_m(t-\tau) + \sin\omega_m\tau - \sin\omega_m t\right] & , \quad \frac{T}{2} \le t \le T \end{cases} \tag{B-1}$$

where the exact representation for θ_d during the turn-around time has been neglected.

Referring to (18), the peak-to-peak frequency deviation in Hz is

$$B = \frac{1}{2\pi}\left[2D\left(b + \frac{aT}{4}\right)\right] \quad . \tag{B-2}$$

Using (18) and (B-2), (B-1) becomes

$$\theta_d(t,\tau) = B\pi \begin{cases} \left(\frac{4\tau P_t}{T}\right)t + \frac{P_s}{\omega_m}\left[\sin\omega_m(t-\tau) + \sin\omega_m\tau - \sin\omega_m t\right] & , \quad 0 \le t \le \frac{T}{2} \\ \left(-\frac{4\tau P_t}{T}\right)(t-T) + \frac{P_s}{\omega_m}\left[\sin\omega_m(t-\tau) + \sin\omega_m\tau - \sin\omega_m t\right] & , \quad \frac{T}{2} \le t \le T \end{cases} \tag{B-3}$$

where

$$P_t \triangleq 1 - P_s \quad .$$

$100P_s$ is the percentage of sinusoidal modulation
and $100P_s$ is the percentage of triangular modulation.

Using (B-3) in (11) we have for the Fourier coefficients

$$c_k = \frac{1}{T}\int_0^{T/2} e^{jB\pi\left\{\left(\frac{4P_t\tau}{T}\right)t + \frac{P_s}{\omega_m}\left[\sin\omega_m(t-\tau) + \sin\omega_m\tau - \sin\omega_m t\right]\right\}} e^{-jk\omega_m t}\, dt$$

$$+ \frac{1}{T}\int_{T/2}^{T} e^{jB\pi\left\{-\left(\frac{4P_t\tau}{T}\right)t + \frac{P_s}{\omega_m}\left[\sin\omega_m(t-\tau) + \sin\omega_m\tau - \sin\omega_m t\right]\right\}} e^{-jk\omega_m t}\, dt \tag{B-4}$$

Using a change of variable, $t_1 = (t - T/2)$, on the second integral and using the approximation:

$$[\sin \omega_m(t-\tau) - \sin \omega_m t] \approx (\omega_m \tau) \sin (\omega_m t - \tfrac{\pi}{2}) \ , \ \tau << T$$

(B-4) becomes

$$c_k = \frac{1}{T} e^{jB\pi P_s \sin \omega_m \tau} \int_0^{T/2} e^{jB\pi \left\{ (\frac{4P_t \tau}{T})t + P_s \tau \sin (\omega_m t - \frac{\pi}{2}) \right\}} e^{-jk\omega_m t} \, dt$$

$$+ \frac{(-1)^k}{T} e^{jB\pi [2P_t \tau + \frac{P_s}{\omega_m} \sin \omega_m \tau]} \int_0^{T/2} e^{-jB\pi \left\{ (\frac{4P_t \tau}{T})t + P_s \tau \sin (\omega_m t - \frac{\pi}{2}) \right\}} e^{-jk\omega_m t} \, dt \qquad \text{(B-5)}$$

Using a change of variable, $\theta = (2\pi/T)t$, and the approximation $\sin \omega_m \tau = \omega_m \tau$ for $\tau << T$, (B-5) reduces to

$$c_k = \frac{1}{2} e^{j(\frac{\pi}{2})P_s x} \left\{ Y[(\tfrac{\pi}{2} P_s x), (k - P_t x)] + (-1)^k e^{j\pi P_t x} Y[(-\tfrac{\pi}{2} P_s x), (k + P_t x)] \right\} \qquad \text{(B-6)}$$

where

$$Y(z,v) \triangleq \frac{1}{\pi} \int_0^{\pi} e^{-j[z \cos \theta + v\theta]} d\theta \qquad \text{(B-7)}$$

and

$$x \triangleq 2B\tau \quad . \qquad \text{(B-8)}$$

$Y(z,v)$ becomes $J_v(-z)$ when v is an integer.

APPENDIX C

Fourier Coefficients For Triangle Plus Cube-Law Modulation

Using (6), (22), (28) and (29), the difference phase is

$$\theta_d(t,\tau) = \begin{cases} (Dc\tau)t + (Dd\tau)\left[(t - \frac{T}{4})^3 + (\frac{T}{4})^3\right] & , \quad 0 \le t \le \frac{T}{2} \\ (-Dc\tau)(t-T) + (-Dd\tau)\left[(t - \frac{3}{4}T)^3 - (\frac{T}{4})^3\right] & , \quad \frac{T}{2} \le t \le T \end{cases} \tag{C-1}$$

where the exact representation of θ_d during the turn-around time has been neglected and the following approximations have been used

$$\left[t - (\frac{T}{4} + \tau)\right]^3 \simeq (t - \frac{T}{4})^3 - 3(t - \frac{T}{4})^2 \quad , \quad \tau << \frac{T}{4} \tag{C-2}$$

and

$$\left[t - (\frac{3}{4}T + \tau)\right]^3 \simeq (t - \frac{3}{4}T)^3 - 3(t - \frac{3}{4}T)^3\tau \quad , \quad \tau << \frac{3}{4}T \quad . \tag{C-3}$$

The approximations are valid for our problem of interest i.e. when $\tau << T$. Substituting (C-1) into (11), the Fourier coefficients are

$$c_k = \frac{1}{T}\int_0^{T/2} e^{j\{(Dc\tau)t + (Dd\tau)\left[(t - \frac{T}{4})^3 + (\frac{T}{4})^3\right]\}} e^{-jk\omega_m t}\, dt + \frac{1}{T}\int_{T/2}^{T} e^{-j\{(Dc\tau)(t-T) + (Dd\tau)\left[(t - \frac{3}{4}T)^3 - (\frac{T}{4})^3\right]\}} e^{-jk\omega_m t}\, dt. \tag{C-4}$$

Using the change in variable, $t_1 = T-t$, on the second integral, (C-4) becomes

$$c_k = \frac{2}{T}\int_0^{T/2} e^{j\{(Dc\tau)t + (Dd\tau)\left[(t - \frac{T}{4})^3 + (\frac{T}{4})^3\right]\}} \cos(k\omega_m t)\, dt \quad . \tag{C-5}$$

Using the change of variable $\theta = (2\pi/T)t$, this reduces to

$$c_k = \frac{1}{\pi}\int_0^{\pi} e^{j\{(\frac{Dc\tau T}{2\pi})\theta + (Dd\tau)(\frac{T}{2\pi})^3[(\theta - \frac{\pi}{2})^3 + (\frac{\pi}{2})^3]\}} \cos(k\theta)d\theta \ . \qquad \text{(C-6)}$$

Referring to (30), the peak-to-peak frequency deviation in Hz is

$$B = \frac{1}{2\pi}\{2D[d(\frac{T}{4})^3 + c(\frac{T}{4})]\} \ . \qquad \text{(C-7)}$$

Using (30) and (C-7), (C-6) becomes

$$c_k = \frac{1}{\pi}\int_0^{\pi} e^{j\{P_t\theta + P_c(\frac{2}{\pi})^2[(\theta - \frac{\pi}{2})^3 + (\frac{\pi}{2})^3]\}x} \cos(k\theta)d\theta \qquad \text{(C-8)}$$

when

$$x \triangleq 2B\tau \qquad \text{(C-9)}$$

$$P_t \triangleq 1 - P_c \qquad \text{(C-10)}$$

$100P_c$ is the percentage of cube-law modulation, $100P_t$ is the percentage of triangular modulation, x is the normalized round-trip time delay between the fuze and the target, and B is the peak-to-peak frequency deviation (Hz).

APPENDIX D

Percentage of Modulation Required For Equivalent Sinusoidal and Cube-Law Nonlinearity

For triangle plus sinusoidal nonlinearity, using (16) and (17), the modulating waveform is

$$m(t) = at + b \sin \omega_m t \quad , \quad |t| \leq \frac{T}{4} \tag{D-1}$$

where the t = 0 reference has been shifted by T/4 for convenience. Then approximating the sinusoidal nonlinearity of (D-1) by the first two terms of the Taylor series we have

$$m(t) = (a + b\omega_m)t - \frac{1}{6} b(\omega_m t)^3 \quad , \quad |t| \leq \frac{T}{4} \quad . \tag{D-2}$$

Identifying (D-2) with (37) we have

$$k_3 = (a + b\omega_m) \tag{D-3}$$

and

$$k_4 = \frac{1}{6} b\omega_m{}^3 \quad . \tag{D-4}$$

For triangle plus cube-law nonlinearity, using (27), (28) and (29), the modulating waveform is

$$m(t) = ct + dt^3 \quad , \quad |t| < \frac{T}{4} \tag{D-5}$$

where the t = 0 reference has been shifted by T/4. Identifying (D-5) with (36) we have

$$k_1 = c \tag{D-6}$$

$$k_2 = -d \quad . \tag{D-7}$$

It is required that $k_1 = k_3$ and $k_2 = k_4$ for these two types of nonlinear modulation to be equivalent. Thus, (D-3) through (D-7) becomes

$$c = a + b\omega_m = a + \frac{2\pi b}{T} \tag{D-8}$$

$$d = -\frac{1}{6} b\omega_m{}^3 = -\frac{1}{6} b \left(\frac{2\pi}{T}\right)^3 \quad . \tag{D-9}$$

Solving (D-8), (D-9), (18) and (19) simultaneously for P_C in terms of P_S we have

$$P_C = \frac{-\frac{1}{6}\left(\frac{\pi}{2}\right) P_S}{\left(1 - P_S + P_S \frac{\pi}{2}\right)\left(\frac{2}{\pi}\right)^2 - \frac{1}{6}\left(\frac{\pi}{2}\right) P_S} \qquad \text{(D-6)}$$

where $100P_C$ is the percentage of cube-law nonlinearity and $100P_S$ is the percentage of sinusoidal nonlinearity.

Equation (D-6) can be arranged into a more useful form

$$P_C = \frac{-[1/6(2/\pi)]^3 P_S}{1 - \dfrac{P_S}{\dfrac{6(2/\pi)^3}{6(2/\pi)^2(1-2/\pi)-1}}} \approx \frac{-0.64596\ P_S}{1 - (P_S/13.304)} \qquad \text{(D-7)}$$

which can be approximated by

$$P_C \approx -0.646 P_S \quad , \quad |P_S| < 1. \qquad \text{(D-8)}$$

REFERENCES:

1. Helstrom, C.W., Statistical Theory of Signal Detection, Pergamon Press, 1968.

2. Skolnick, M., Editor, Radar Handbook, McGraw-Hill, 1970.

3. Rowe, H.E., Signals and Noise in Communication Systems, Van Nostrand, 1965.

4. Rihaczek, A.W., Principles of High Resolution Radar, McGraw-Hill, 1969.

5. Peperone, S.J., "Analysis of the C-Class Fuzing Systems," Harry Diamond Laboratories Technical Report No. TR-914, 1961.

6. Tozzi, L.M., "Resolution in Frequency-Modulated Radars," Ph.D. Dissertation, University of Maryland, 1972.